

This is an Open Access document downloaded from ORCA, Cardiff University's institutional repository:<https://orca.cardiff.ac.uk/id/eprint/146508/>

This is the author's version of a work that was submitted to / accepted for publication.

Citation for final published version:

Hawi, Sara, Goel, Saurav, Kumar, Vinod, Pearce, Oliver, Nishio Ayre, Wayne and Ivanova, Elena P. 2022. Critical review of nanopillar-Based mechanobactericidal systems. *ACS Applied Nano Material* 5 (1) , pp. 1-17. [10.1021/acsnm.1c03045](https://doi.org/10.1021/acsnm.1c03045)

Publishers page: <http://dx.doi.org/10.1021/acsnm.1c03045>

Please note:

Changes made as a result of publishing processes such as copy-editing, formatting and page numbers may not be reflected in this version. For the definitive version of this publication, please refer to the published source. You are advised to consult the publisher's version if you wish to cite this paper.

This version is being made available in accordance with publisher policies. See <http://orca.cf.ac.uk/policies.html> for usage policies. Copyright and moral rights for publications made available in ORCA are retained by the copyright holders.



1 **Critical Review of Nanopillar-Based Mechano-Bactericidal Systems**

2

3 *Sara Hawi^a, Saurav Goel^{b,c,d*}, Vinod Kumar^{a,e}, Oliver Pearce^f, Wayne Nishio Ayre^g and*

4 *Elena P. Ivanova^h*

5 ^a Cranfield University, Cranfield, MK43 0AL, UK

6 ^b London South Bank University, 103 Borough Road, London, SE10 AA, UK

7 ^c Indian Institute of Technology Guwahati, Guwahati, 781039, India

8 ^d University of Petroleum and Energy Studies, Dehradun, 248007, India

9 ^e Indian Institute of Technology Delhi, Hauz Khas, New Delhi 110016, India

10 ^f Milton Keynes University Hospital, Milton Keynes, MK6 5LD, UK

11 ^g Cardiff University, Cardiff, CF14 4XY, UK

12 ^h School of Science, RMIT University, Melbourne, Victoria 3000, Australia

13 **Corresponding Author**

14 *E-mail: goeLs@Lsbu.ac.uk

15 **Abstract**

16 The rise of multidrug resistant bacteria is the biggest threat to human health globally as
17 described by the World Health Organization (WHO). Mechano-bactericidal surfaces provides
18 a sustainable approach to address this concern by eradicating pathogens, especially bacteria,
19 "right-at-the-point" of first contacting the surface. However, the lack of a "design to
20 manufacture" approach due to our limited understanding of the mechano-bactericidal
21 mechanism has impeded engineering optimization to develop scalable exploitation routes in
22 various healthcare applications. It can be argued that the reason, most particularly, is the

1 limitations and uncertainties associated with the current instrumentation and simulation
2 capabilities which has led to several streams of test protocols. This review highlights the current
3 understanding on the mechano-bactericidal mechanisms in light of the contributing factors and
4 various techniques which are used to postulate these mechanisms. The review offers a critique
5 on the variations observed on how nanostructured surfaces found in literature have been
6 evaluated such that the test protocols and the outcomes are incomparable. The review also
7 shows a strong need of developing more accurate models of a bacterium as the currently
8 reported experimental data is insufficient to develop bacteria's material models (constitutive
9 equations). The review also alludes to the scarcity of direct experimental evidence of the
10 mechano-bactericidal mechanism suggesting a strong need for further in-situ monitoring as a
11 future research direction.

12 **Keywords:** Mechano-bactericidal; nanostructured surfaces; biomimicry; nature-inspiration;
13 engineering biology

14

15 Antibiotics are crucial in treating bacterial infections. However, the misuse of antibiotics has
16 empowered bacteria to develop resistance by, most prevalently but not exclusively, secreting a
17 shielding biofilm to prevent therapeutic access. Presently, antibiotic resistance (ABR), a subset
18 of antimicrobial resistance¹ is an eminent threat to human health and human quality of life
19 globally. As the development of novel antibiotics and antimicrobials has been diminishing,
20 new approaches to combat this rapidly growing issue have become a necessity². Moreover,
21 treatment without prevention is insufficient, especially with regards to biomaterial-associated
22 infections, as this can dictate the fate of implant surgeries by tipping the scale in favor of
23 bacteria in the "race for the surface" against eukaryotic cells³. Clinical statistics suggests that
24 the percentage of post-operative infections of orthopedic implants ranges between 0.7 % and

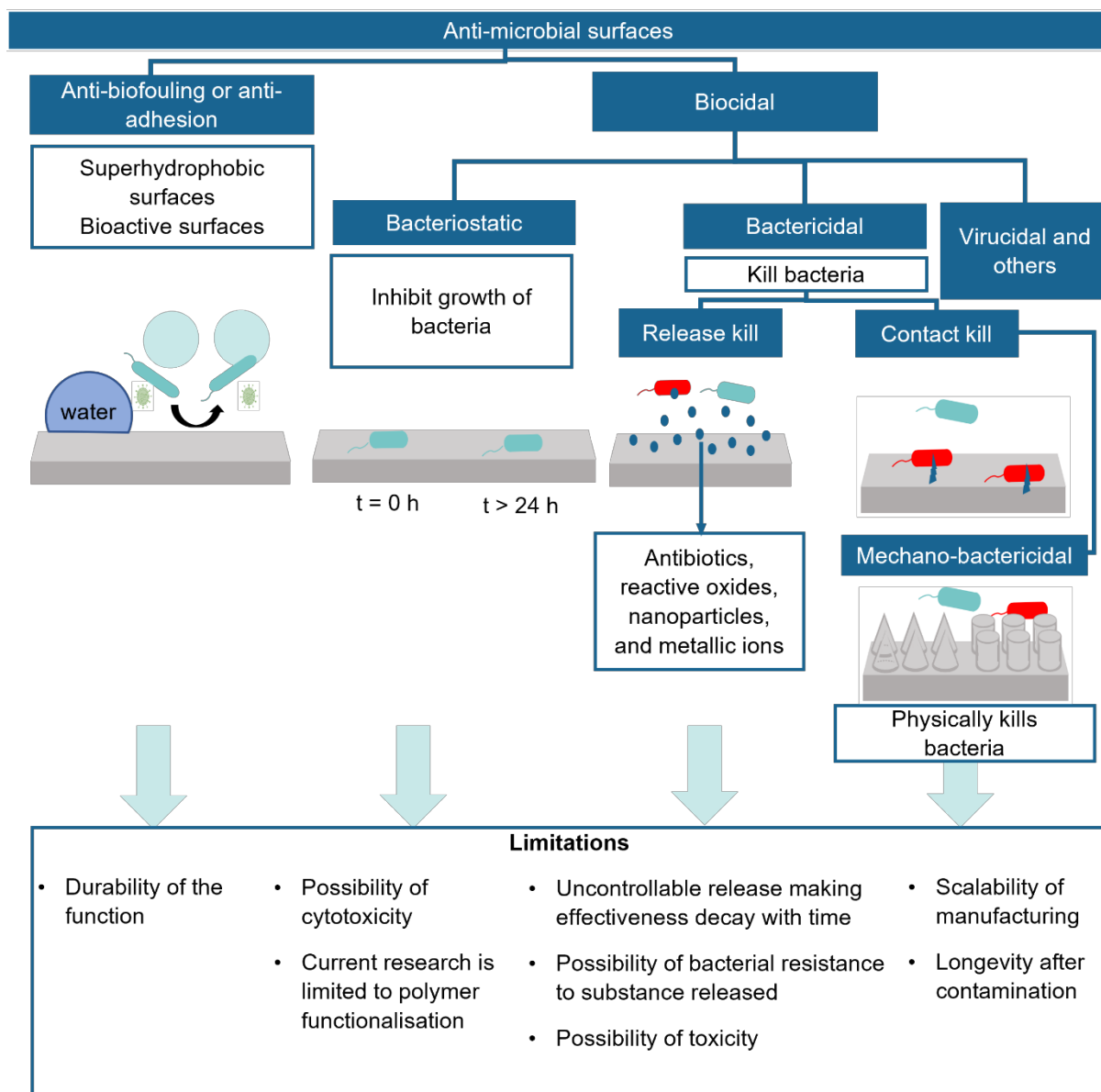
1 4.2 %.⁴⁻⁶ This percentage can be as high as 30% for complex trauma cases^{7,8} as the surfaces of
2 these implants are at high risk of bacterial contamination. The ABR of pathogenic bacteria such
3 as *Staphylococci* and *Streptococci*, among others, renders existing antibiotic treatments for
4 post-operative infections futile, with resistance starting to emerge for last resort antibiotics such
5 as vancomycin⁹ (widely used in orthopedics), polymyxin B and colistin.¹⁰ Protective biofilms
6 can form within hours of implantation and therefore agile preventative methods are required,
7 which are being currently explored. Such methods have been directed towards preventing
8 bacterial contamination and biofilm formation by modifying the surfaces using various
9 techniques which are termed as "anti-bacterial". Contrary to the common practice in non-
10 biology (especially engineering) related fields, the term anti-bacterial is not exchangeable with
11 anti-microbial, but a subset of it. Herein, a classification is offered (see fig 1) to highlight anti-
12 microbial surfaces by their specific functions. Based on this classification, anti-microbial
13 surfaces can be categorized as follows:

- 14 • Anti-biofouling or anti-adhesion surfaces that repel microbes (i.e., bacteria, viruses,
15 fungi) and prevent them from adhering to the surface, and
- 16 • Biocidal surfaces that can kill or suppress the growth of microbes.

17 Biocidal surfaces can be further divided as (i) bacteriostatic, which can prevent the
18 proliferation of bacteria, (ii) bactericidal which can kill the bacteria either through release or
19 contact kill mechanisms, and (iii) antiviral or virucidal surfaces that are lethal to viruses.

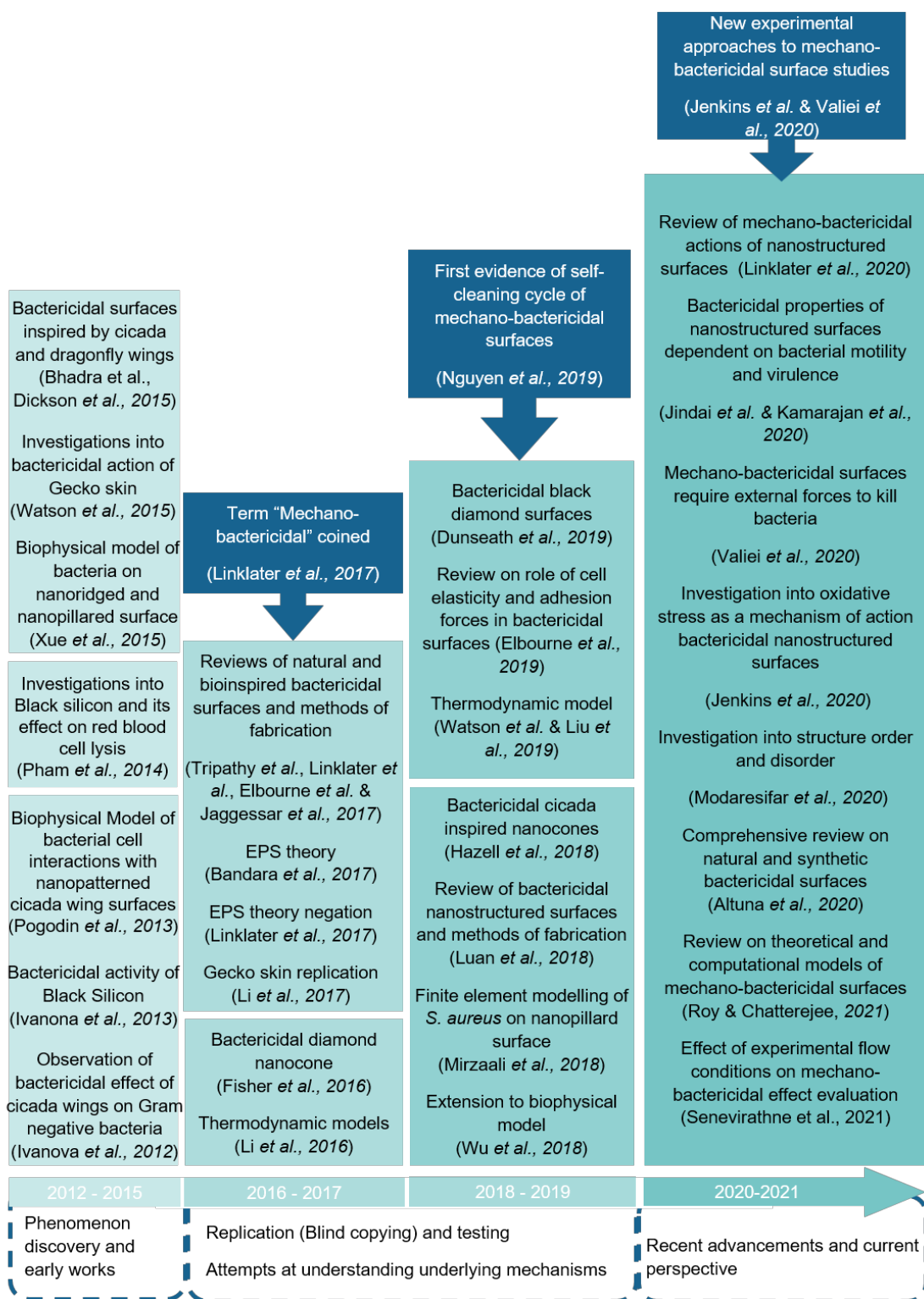
20 Focusing on bactericidal surfaces, release kill and contact kill surfaces have slight differences
21 between them. Release kill surfaces are those that cause ozone exposure triggered by metallic
22 ions^{11,12} (ionic silver, ionic copper, graphene nanosheets, carbon nanotubes etc.) or that can
23 release antimicrobials from the surface into the surrounding fluid to kill the bacteria. Contact
24 kill surfaces are those which can kill the bacteria merely by their physical presence either by
25 virtue of the surface chemistry (coating, immobilized antimicrobial agents etc.) or their

1 surface topography (physical geometry, nanostructure, nanotexture, etc.), often referred to as
 2 mechano-bactericidal.



3
 4 **Figure 1:** Positioning mechano-bactericidal surfaces in the broader antimicrobial landscape.

5 Mechano-bactericidal surfaces have gained significant interest recently (Fig. 2) as potential
 6 anti-bacterial biomaterial surfaces due to their premise of transferability to different
 7 biomaterials. The bactericidal mechanism(s) behind their action remains unclear due to
 8 complexities that accompany bacteria-surface experimental investigations and a lack of
 9 uniformity in the reported data.



1

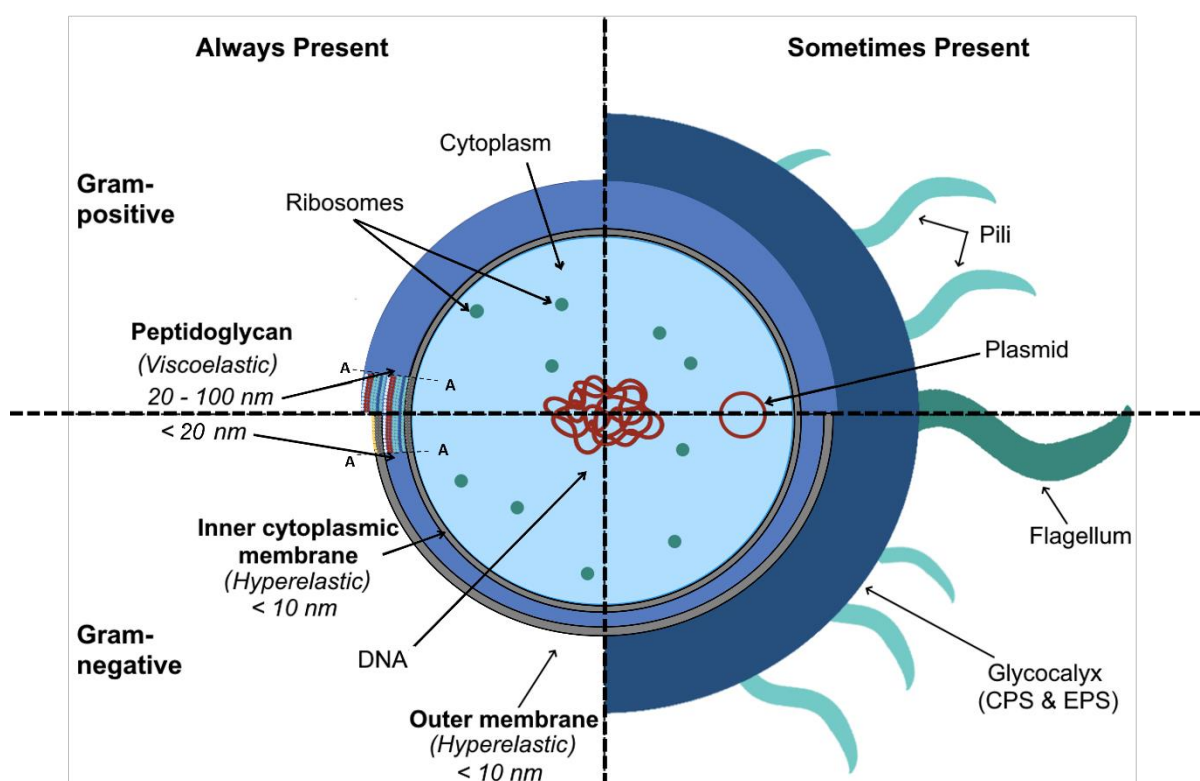
2 **Figure 2:** Timeline showing progressive learning about the bactericidal surfaces based on the
 3 topography of cicada and dragonfly wings.

4 Conflicting correlations have, thus, been made between bactericidal efficiency and: (i)

5 surface water contact angle, (ii) surface roughness, and (iii) nanostructure interspacing,

1 among others. It is however categorically established that the mechanism is independent of
2 surface chemistry⁴⁸ and relies on the mere topography of the surface, hence the prefix
3 "mechano". Moreover, it has been suggested that the biocidal action can be expanded to
4 affect other microbes i.e., viruses^{38,49} and yeast⁵⁰ cells.

5 In this mechano-bactericidal killing approach, the understanding of the bacterium's anatomy
6 (shown in Fig. 3) becomes increasingly important.



7
8 **Figure 3:** The anatomy of bacteria. Section A-A depicts the basic structure of the
9 peptidoglycan, the cytoplasmic membrane, and the outer membrane. The grey circles represent
10 the lipid bilayer, the turquoise (light blue circles) represent the alternating units of N-
11 acetylglucosamine and Nacetylmuramic acid, with the N-acetylmuramic acid residues cross-
12 linked to peptides. The yellow circles represent the lipopolysaccharides. CPS and EPS stand
13 for capsular polysaccharids and extracellular polymeric matrix respectively.

1 The main structural elements constituting bacteria are the cytoplasm, the peptidoglycan and
2 the membranes (cytoplasmic and outer). The cytoplasm is a matrix that is composed mostly
3 of water (80%) and contains enzymes, nutrients, wastes, gases, ions and cellular components
4 such as the ribosomes, plasmid (if any), the bacterial DNA, etc. It has been reported to
5 behave as a glass-forming fluid in some studies⁵¹, but generally its material properties remain
6 uncharacterized. The peptidoglycan is a very robust protective layer that is made up of
7 repeating disaccharides of N-acetylmuramic acid and N-acetylglucosamine that are linked by
8 $\beta(1-4)$ glycosidic linkages⁵². A recent report⁵³ claims that the latter exhibits viscoelastic
9 behavior when subjected to indentation load under an atomic force microscope (AFM).

10 The cytoplasmic membrane, or inner membrane of a bacterium, is a phospholipid bilayer
11 whereas the outer membrane (in case of Gram-negative bacteria) is principally made up of
12 lipopolysaccharide. Measuring the mechanical properties of the individual components of the
13 bacterial cell wall continues to be a great challenge due to the cellular complexity. However,
14 cellular membranes consisting of lipid bilayers and lipopolysaccharides have been reported to
15 behave elastically under large deformations⁵⁴, making them hyperelastic materials.

16 In the next sections, the review critiques the sources of bias introduced by the experimental
17 techniques used to study nanostructured mechano-bactericidal surfaces and their mechanisms.
18 Accordingly, the review presents the settled understanding on the various bactericidal
19 mechanisms of such surfaces and the factors influencing the efficiency of the bactericidal
20 activity. It also offers a discussion and an open invitation for leading groups in the field to
21 consider experimental approaches and standardized techniques to eliminate bias and
22 circumvent uncertainty to improve the test protocols for evaluating the mechano-bactericidal
23 surfaces.

1 **Mechano-bactericidal mechanisms**

2 In the quest to elucidate the mechanism(s) underlying mechano-bactericidal activity, two
3 research approaches have been adopted which are based either on experimental data or
4 continuum simulations. In the next sections, the techniques used to evaluate bactericidal
5 surfaces have been discussed, followed by the mechanisms revealed by these experimental
6 approaches, the mechanisms revealed by simulation approaches and the factors playing into
7 the effect of mechano-bactericidal structures. The limitation of experimentation and
8 simulations will both be discussed in their prospective sections.

9 **Techniques used to evaluate bactericidal surfaces and bacteria-surface** 10 **interactions**

11 As bacteria-surface interactions remain largely unknown in the light of evolving experimental
12 procedures, a range of techniques have been used to study bactericidal surfaces mostly at
13 discrete time points.

14 To study this interaction, mechano-bactericidal surfaces are first incubated with a volume of
15 bacterial suspension (*i.e.*, a nutrient-rich broth containing bacteria). This can be done using
16 one of the three main set-ups presented in Fig. 4 (a); the overlay or drop-test method where a
17 droplet with large volume is deposited onto the nanostructured surface,⁵⁵ the spray method
18 where the bacterial suspension is sprayed over the surface,⁵⁶ and the immersion method
19 where the nanostructured sample is fully immersed in the bacterial suspension.⁵⁷ The overlay
20 and spray methods introduce surface tension at the perimeter of the droplets which might
21 induce an external force that is able to drive the bacteria towards the nanostructures, hence
22 stimulating a high bactericidal reaction (Fig. 5 (d)). Since the overlay method consists of one
23 large drop instead of smaller dispersed droplets as in the case of spraying, it is more suitable
24 to use when evaluating mechano-bactericidal surfaces. The high bactericidal effect-inducing
25 surface tension at the droplet perimeter can be eliminated from consideration when analyzing

1 the results. These two methods cannot be used to test the functionality of the surfaces for long
2 periods of time as they are prone to evaporation. The immersion method, on the other hand,
3 provides the possibility of long duration functional analysis, continuous durability analysis (>
4 24 h), studying potential self-cleaning cycles of mechano-bactericidal surfaces,³¹ and
5 eliminating surface tension-inducing bubbles by using dynamic incubation.⁵⁸

6 To assess and compare the bactericidal performance of various nanopatterns, it is critical to
7 consistently test the *non-specific* bacterial response using the same type strains and growth
8 conditions. However, due to vast diversity of bacteria, which is reflected in differences of the
9 bacterial cell wall composition and thickness,^{59,60} wettability, and *specific* host interactions
10 of clinical isolates, different strains that belong to the same species, may respond differently
11 to the same nanopattern.^{61,62}

12 One important aspect to study, which is largely absent in literature, is the protein
13 preconditioning of mechano-bactericidal surfaces, especially when considering end
14 applications such as biomedical implants. As these implants are inserted into the body, the
15 first thing that comes into contact with them is blood and this results in instantaneous
16 formation of a protein film. This protein film might mask or reduce the effect of the
17 mechano-bactericidal surface as it can fill the spacings between the nanostructures rendering
18 them ineffective. That is why, it is of utmost importance to study serum preconditioning of
19 the surfaces prior to incubation with bacteria. Understanding how that protein film forms on
20 mechano-bactericidal surfaces can help the structure optimization process to be more
21 efficiently bactericidal.

22 After incubation, the first objective to seek when studying a mechanically designed
23 bactericidal surface is to evaluate the effectiveness of this surface towards a specific bacterial
24 strain. For that, it would be beneficial to know the number of bacteria attached to the surface
25 (dead and alive). Additionally, it is imperative to ensure that the surface is bactericidal by

1 detecting the count of dead bacteria over a timespan and, to quantitatively determine its
2 bactericidal efficiency expressed as:

$$3 \quad \eta_{\text{bactericidal}}(\%) = \left(\frac{A - B}{B} \right) \times 100 \quad (1)$$

4
5 where A is the number of dead bacteria on the test sample surface and B is the number of
6 dead bacteria on the reference sample surface.

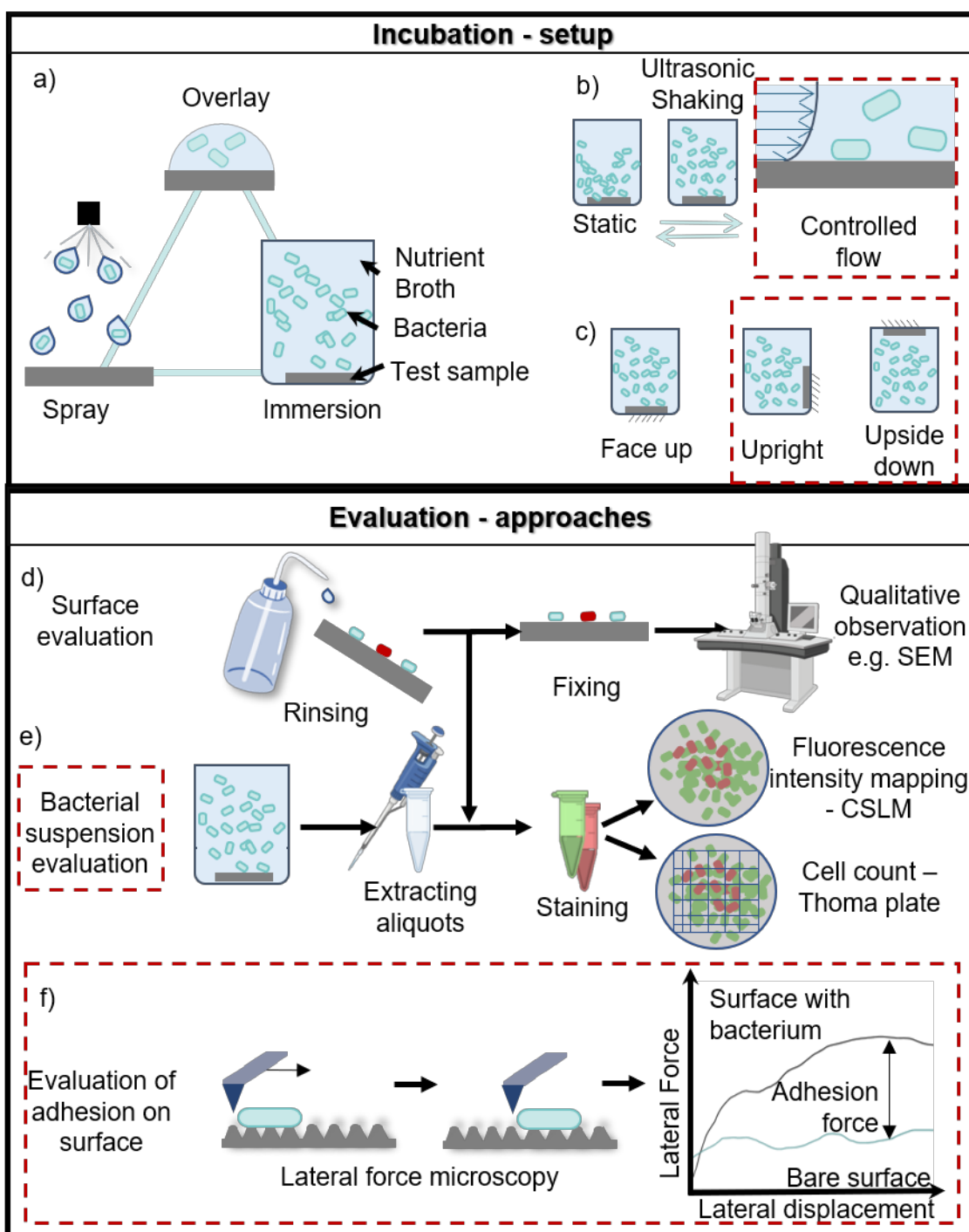
7 Previously, bactericidal efficiency has been evaluated using the colony counting or colony
8 forming unit method (CFU). It is a method used to quantify the number of colonies that can
9 grow in a nutrient medium (agar) from a swab of bacteria-exposed test surface or after rinsing
10 the bacterial test surface and replating the suspension medium. This method can indirectly
11 quantify the number of live and attached bacteria on the test surface.

12 However, the CFU method does not guarantee complete removal of all bacteria from the
13 surface and often times, the technique for removal (e.g., sonication, enzyme) may cause cell
14 death. Additionally, CFU underestimates the true killing efficiency of the surface as it fails to
15 account for the number of dead bacteria on the surface and the dead bacteria that could have
16 been released out onto the suspension after death^{41,63}. This method evaluates the ability of a
17 bacteria to attach and proliferate on the surface rather than the killing ability of a surface.

18 That is why this technique is better suited to evaluate the anti-biofouling functionality rather
19 than the bactericidal efficiency of a test surface, unless accompanied by other forms of
20 viability quantification such as Live/dead staining.

21 Although theoretically, there are distinct definitions of bacteriostatic versus bactericidal
22 surfaces, in practice they are ill-defined. For instance, when discussing bacterial killing
23 agents or antibiotics, a general consensus is that in an incubation duration of 18-24 hours, if
24 the agent is able to kill 90-99% bacteria, it is called bacteriostatic and if it is able to kill
25 >99.9% bacteria, it is considered bactericidal.⁶⁴ This is to account for the *in vivo* factors in

1 infection with time. However, when discussing bacteria killing surfaces, the quantitative
 2 value is not specified for the designation between bactericidal and bacteriostatic. This
 3 constitutes an empirical need to identify the clinically relevant threshold above which the rate
 4 of bacterial death is quicker than the multiplication of bacteria in the deep prosthetic surgical
 5 site infection. Understanding this threshold will allow for the consistent labelling of
 6 bactericidal surfaces in the biomedical field.



1 **Figure 4:** The incubation set-up including a) the method and volume of bacterial suspension
2 contact with the sample surface: the overlay, spray and immersion methods , b) the flow
3 conditions during incubation: static and dynamic comprising ultrasonic shaking and
4 controlled flow, c) the sample orientation: face up, upright and upside down, d) Surface
5 evaluation by rinsing, e) the bacterial suspension live/dead cell count methods, f) the
6 evaluation of bacterial adhesion on nanostructured surfaces using lateral force microscopy.
7 The dotted red rectangle denotes the areas that are least explored or unexplored as of yet.

8 The durability of the bactericidal function is under question and experimental tests can be
9 intriguingly used to understand the fate of bacteria after they become non-viable on the
10 surface. Intuitively, one would think that the non-viable bacteria would remain in the pits of
11 the mechano-bactericidal structured surface and constitute a means of adhesion and nutrition
12 for newly adhering bacteria. Another possible fate of the non-viable bacteria however would
13 be the detachment and return to bulk fluid. In the latter case, considering the number of non-
14 viable bacteria present in the bulk liquid would be important to quantify the bactericidal
15 efficiency of the test surface. It is also vital to quantify the time of the killing of a bacterium
16 to judge the degree of surface's lethality against high bacterial loads.

17 The experimental techniques used to address these points are relatively straightforward. For
18 instance, the number of bacteria adhering to the surface and/or present in the bulk liquid can
19 be evaluated by different types of assays in conjunction with labelling methods such as
20 fluorescent staining, dye staining and several others that would allow the differentiation
21 between live and dead bacterial cells as presented in Fig. 4 (e). Most commonly, Confocal
22 Laser Scanning Microscopy and BacLight viability testing kits (Syto9™ fluorescent green &
23 Propidium iodide fluorescent red) are used for live/dead assays as shown in Fig. 4 (a).

24 Through this method, Nguyen *et al.*³¹ tracked *P. aeruginosa* bacterial cells on silicon
25 mechano-bactericidal surfaces, observing their detachment as presented in Fig. 5 (b). This
26 test method is based on the assessment of the membrane permeability of bacteria. Syto9™ is
27 a dye that can enter live and dead cells alike, while Propidium iodide or PI can only stain
28 dead cells. There have been a few problems associated with the use of these dyes in

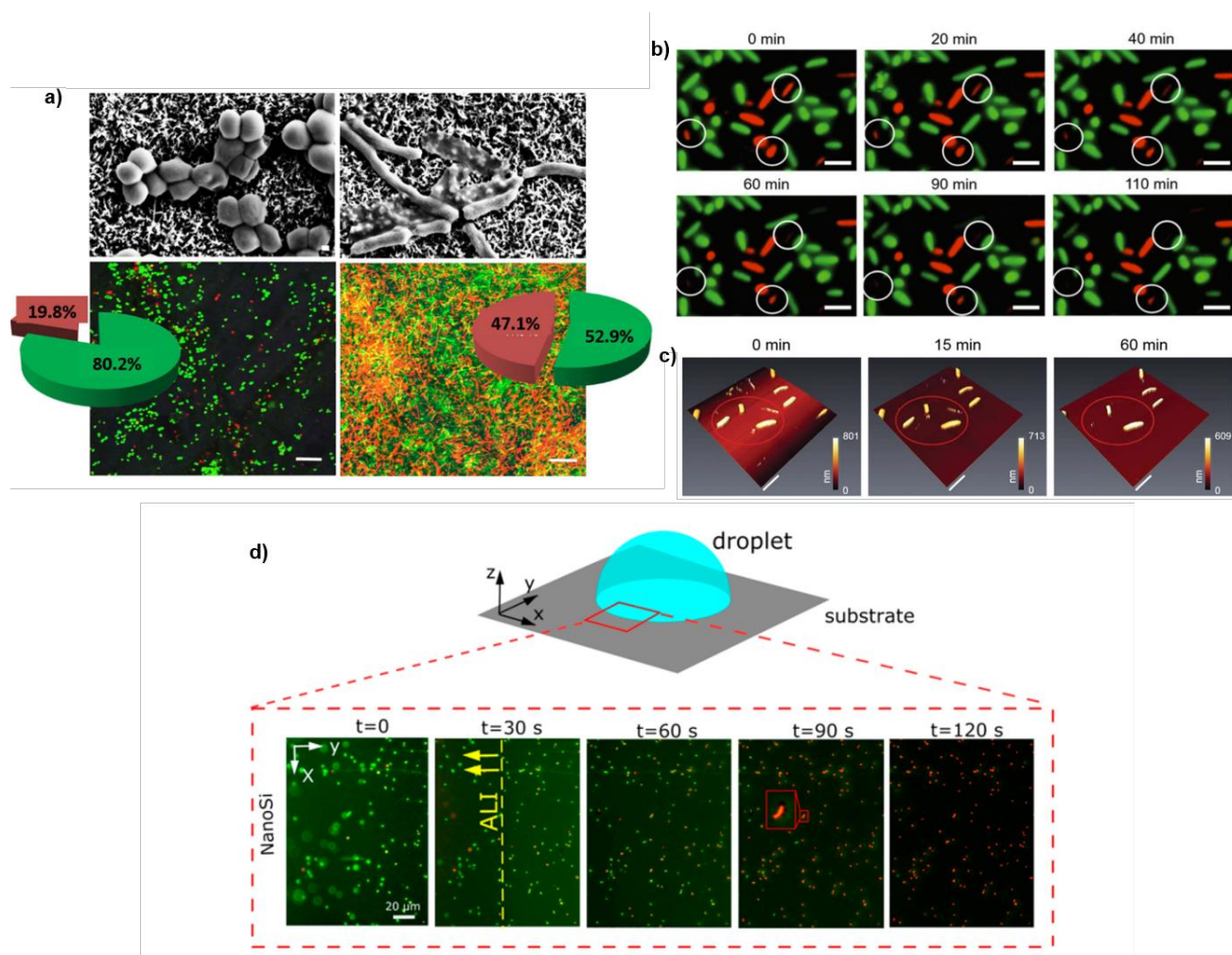
1 determining cell viability, for instance in dye bleaching due to overexposure, low intensity of
2 PI especially at high dead bacterial loads and orange-yellow coloring of some bacteria which
3 is attributed to the slow permeability of PI after SYTO9 staining. That is why care must be
4 taken while performing measurements with such dyes, by for example quickly and
5 efficiently taking the measurements and closing the microscope shutter in between captures
6 to delay the bleaching effect. Additionally, atomic force microscopy (AFM) was used to
7 quantify this detachment cycle using quantitative imaging mode (QI™) to avoid applying any
8 significant lateral forces to the cells (Fig. 5 c).^{31,65}

9 Another important objective should be to evaluate how bacteria die on the mechano-
10 bactericidal surfaces. As it has been shown by Jenkins *et al.*³³ and Ishak *et al.*,⁶⁶ the number
11 of bacteria dying from penetration does not necessarily equate to the total number of dead
12 bacteria. That is why, to understand what mechanisms are at play in the bactericidal action of
13 the test surface, it is important to quantify the number of bacteria that are dead specifically
14 from penetration or deformation and compare it to the total number of dead bacteria.

15 Bactericidal mechanisms, other than penetration and stretching, that surfaces can be
16 exhibiting should be investigated to see if they are occurring, such as oxidative stress or
17 others. Additionally, the driving force of the mechano-bactericidal activity needs to be
18 investigated. For instance, samples can be incubated in different orientations to evaluate the
19 gravity effect on the bactericidal activity and if it is indeed the driving force for it. The
20 adhesion force between the bacteria and the surface can also be investigated to see whether it
21 is enough to invoke the rupture of the bacterial membrane.

22 Furthermore, bioAFM can be used to quantify the adhesion force between the bacteria and
23 the surface by lateral force microscopy as presented schematically in Fig. 4 (f), and to
24 quantify the elastic properties of the bacterial cell by AFM force spectroscopy through
25 indentation and retraction.⁶⁷⁻⁶⁹

1 These points are harder to address as techniques that could be used to do so require
2 expensive, special and sophisticated equipment and multidisciplinary training. Furthermore,
3 investigating the detailed workings of mechano-bactericidal surfaces ideally requires real-
4 time monitoring and in-depth microbiological investigations. This research area is very
5 fertile, and many basic discoveries are yet to occur. For example, investigation into whether
6 cell death was mediated by ROS on mechano-bactericidal surfaces was only done recently
7 through protein extraction, proteomic analysis and H₂O₂ labelling assays.³³ Cross-sectional
8 observation of surface and bacteria contact performed through SEM-FIB or TEM can aid in
9 analyzing if bacterial membranes are being deformed and penetrated by the nanostructures
10 present on mechano-bactericidal surfaces and to what extent (Fig. 4 (d)).



1

2 **Figure 5:** (a) CLSM images of viable and non-viable *S. aureus* and *P. aeruginosa* on
 3 nanostructured surfaces.⁴⁴ (b) CLSM and (c) AFM tracking of non-viable bacteria on
 4 mechano-bactericidal nano-arrayed surface. Reprinted from ref³¹ by permission of Royal
 5 Society of Chemistry. Copyright 2019.

6 (d) Overlay/drop-test on Nano-Silicon surface:
 7 Viability of bacteria as a function of time as the bacterial droplet is subject to evaporation
 8 (ALI is the air liquid interface). Live cells are green and non-viable cells are red. Reprinted
 9 from ref⁵⁸ by permission of ACS Publications. Copyright 2020.

9 The effects of the flow on attachment and death of bacteria have not been extensively
 10 explored as most experimental studies follow static incubation protocols (see Fig. 4 (b)). On
 11 one hand, the efficiency under static protocols can be underrated compared to the efficiency
 12 in flow conditions. That is because in static conditions, a build-up of bacteria may occur. Yet

1 on the other hand, the efficiency under static protocols can also be overrated as stated by
2 Valiei *et al.*³⁴. They argued that in static conditions, air bubbles present between the surface
3 and the bacteria suspension could expand during microscopic evaluation and induce an
4 external force that drives the killing effect of nanostructures. Whereas in dynamic conditions,
5 these bubbles are simply eliminated by ultrasonic shaking. In fact, static conditions do not
6 mimic reality. In biomedical applications there is fluid flow surrounding biomedical implants.
7 Therefore, the determination of bactericidal efficiency should be done under realistic flow
8 conditions (measured shear flow rate). It is however important to keep in mind that under
9 dynamic conditions, the adhesion of bacteria decreases, and detachment increases compared
10 to static conditions which might affect the results. It is also possible to postulate that under
11 flow conditions, the bacteria experience advective flow which causes their collision with
12 nanopillars with a significant impact force that might increase the killing efficiency.⁷⁰ On the
13 other hand, a recent study by Kamarajan *et al.*⁷¹ has reported an increased adhesion and
14 survival rate for *P. aureuginosa* PAO1 on nanostructured surfaces under flow conditions.
15 They attributed this behavior to the increased secretion of EPS adopted by the bacteria which
16 masked the nanopillar tips. This goes to show that understanding the response of bacteria to
17 mechano-bactericidal surfaces in flow conditions is vital in determining the surfaces' true
18 efficiency. A more detailed discussion of experimentation under flow conditions can be
19 found in a review by Senevirathne *et al.*⁴¹.

20 Additionally, substrate orientation (Fig. 4 (c)) is important to help determine the driving force
21 of the mechanism.

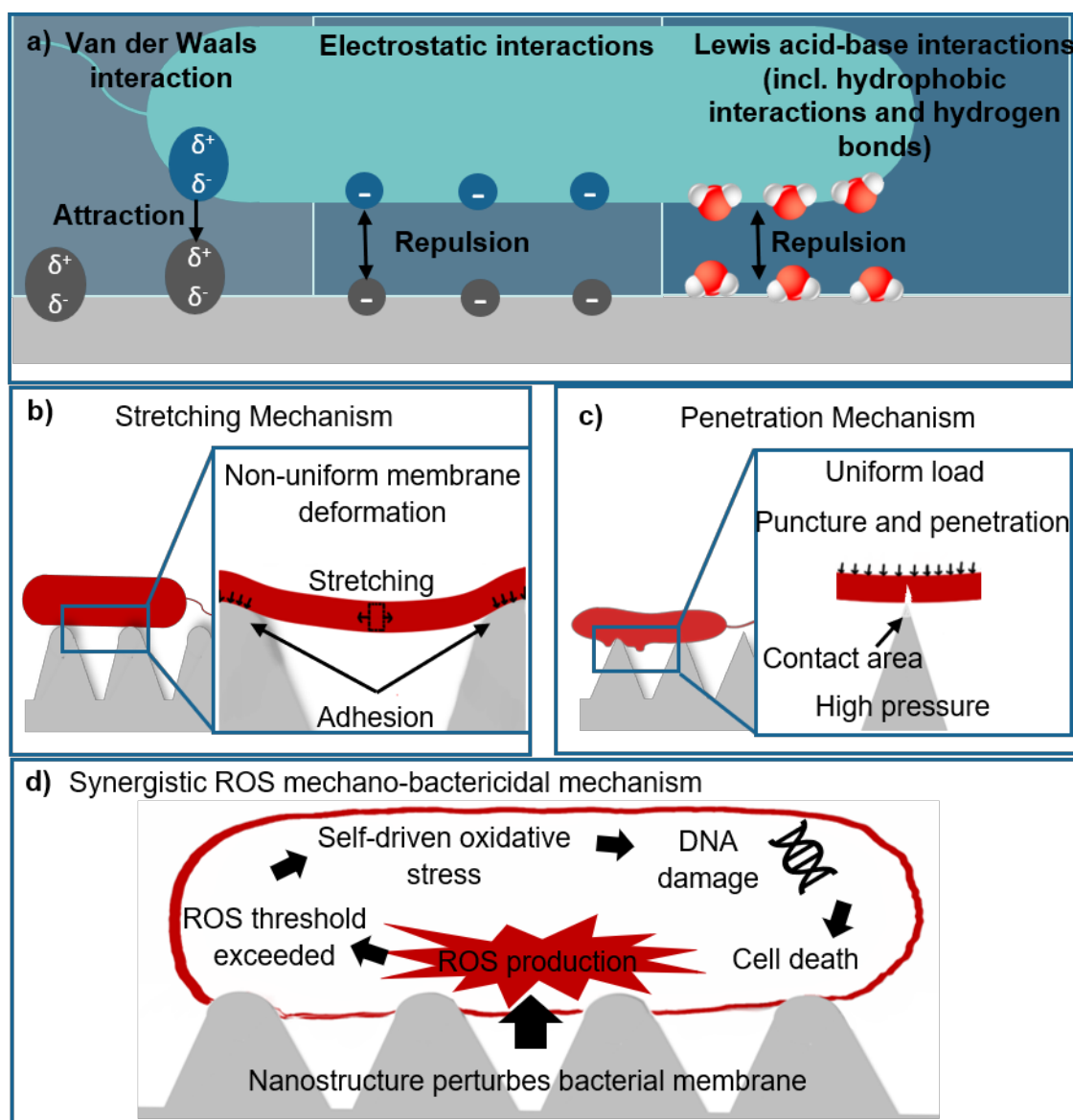
22 A summary of the techniques used to evaluate and investigate mechano-bactericidal surfaces
23 to date highlighting their advantages, limitations, and the errors that could possibly occur by
24 their usage can be found in the supporting information.

25 **Mechanisms revealed from the experimental approaches**

1 Through experimental approaches, nanostructured surfaces gained their reputation as
2 mechano-bactericidal surfaces, independent from chemical effects⁴⁸ as the functionality
3 (bacteria killing ability) was shown to persist across different materials.

4 Early research relied on observations from techniques such as Scanning electron microscopy
5 (SEM) imaging to form the hypothesis that nanostructures puncture bacterial cell walls
6 leading to the release of cytoplasmic fluid (Fig. 6 (c)). This was due to compromised cells
7 taking the shape of the nanopillars, revealed by the SEM images which led to the conclusion
8 that the nanostructures puncture the bacteria. Techniques of evaluation then progressed into
9 methods that can reveal the nanostructure/bacteria interaction through cross-sectional
10 imaging e.g., Focused Ion Beam (FIB). Recently, slice-by-slice FIB-SEM data reconstruction
11 was used to better observe the interaction of nanopillars with single cells⁷² leading to an
12 improvement from the previous postulations. Several hypotheses then emerged, one of which
13 is specific to Gram-negative motile bacteria.¹⁶ This hypothesis suggests that the biocidal
14 activity is mediated by an extracellular polymeric substance (EPS). This mechanism was later
15 refuted as it disregards the fact that the bactericidal effect occurred within a few minutes of
16 contact whereas EPS secretion is thought to take significantly longer (hours to days).^{35,17}

17 Amidst the development of these hypotheses, it was experimentally established that the
18 effusion of intracellular fluid does occur for *Escherichia coli* on nanostructured surfaces
19 using fluorescent proteins.⁷³ This important finding confirmed that rupturing of the bacterial
20 membrane is involved in the bactericidal action presented by the nanostructures.



1

2 **Figure 6:** (a) Factors that may influence the initial bacterial attachment to a solid-liquid
 3 interface adapted from ⁷⁴, (b) The stretching mechanism proposed, (c) The penetration
 4 mechanism based on sharp nanostructures and (d) the synergistic ROS mediated mechano-
 5 bactericidal mechanism.

6 Meanwhile, one of the coauthors Ivanova *et al.*¹⁴ suggested that the bactericidal activity of
 7 nanostructures is actually driven by the mechanical and structural responses of the bacterial
 8 cell as it adheres to the nanostructures. Particularly, these responses create inelastic stress
 9 imposed by the surface nano-topography on the peptidoglycan cell wall and inner membrane

1 of the bacterial cells. Herein, the surface ineffectiveness against Gram-positive bacteria was
2 attributed to the thickness of the peptidoglycan layer in the cell wall as it is four to five times
3 thicker than that of Gram-negative bacteria.⁷⁵ This was named as the "stretching" mechanism
4 (Fig. 6 (b)) and thought to compete the "penetration" mechanism.

5 Exhaustively, all these hypotheses were inferred from indirect evidence from the same
6 experimental approaches (mainly CLSM, SEM and FIB-SEM) with interpretations based on
7 *a priori* knowledge, which introduced a certain bias towards the previously conceived
8 stretching and penetration mechanisms. It is imperative to look at the problem from an
9 alternative perspective proposed here.

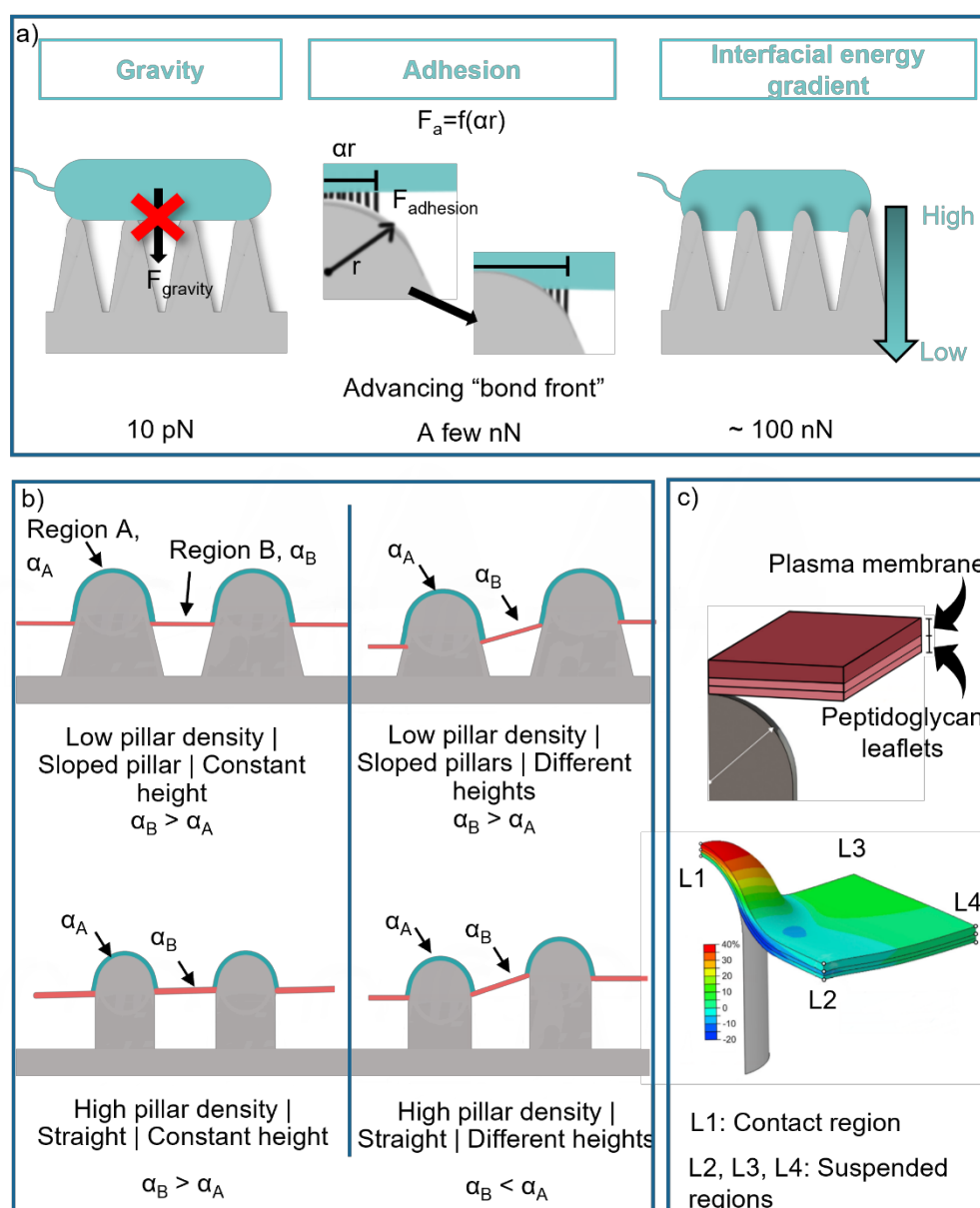
10 A few recent studies have shed light on the shortcomings of the experimental approaches
11 employed in understanding the underlying mechanisms of the mechano-bactericidal effect.
12 One such study by Jenkins *et al.*³³ provided a baseline for a reactive oxygen species (ROS)
13 mediated mechanism as bacteria exposed to the nanostructures (be it Gram-positive or Gram-
14 negative) were found to be oxidatively stressed. This occurs when bacteria are subjected to a
15 lethal stressor which triggers production of ROS as a self-destruction mechanism.⁷⁶ Bacteria
16 can detoxify low levels of reactive oxygen species (except hydroxyl radical) through several
17 protective enzymes (e.g. superoxide dismutase, catalases).⁷⁷ However, if the ROS levels
18 surge above a certain threshold, the death process becomes self-driven and irreversible even
19 if the initial stressor is removed.⁷⁶ This synergistic ROS-mediated mechano-bactericidal
20 mechanism, illustrated in Fig. 6 (d), sheds a new light on the importance of expanding the
21 experimental approach to look beyond the "penetration" or stretching mechanisms. In other
22 words, the mechanism, although shown to be surface chemistry independent, does involve
23 chemistry at a bacterial level contrary to the currently presented pure mechanistic models.

1 Nonetheless, understanding the proposed mechanisms is imperative to evaluate their role in
2 the bactericidal pathway of the nanostructures. "Penetration" as a term has repeatedly been
3 used to explain that the failure of the bacterial membrane in the area that is directly in contact
4 with the nanostructures. However, the term penetration in its essence indicates that stress
5 concentrations leading to fracture occurs at the failure site which in turn requires a very sharp
6 rigid structure. For "penetration" or puncture to mechanically occur, the degree of freedom of
7 the penetrated object should be restricted which is mostly not the case in this scenario of
8 bacteria-nanostructure interaction. Thus, if failure occurs at the apex of the nanopillar, it is
9 due to the local stretching or pressure on the membrane in that region. The question remains
10 as to where the critical action site is within the mechano-bactericidal mechanism and what is
11 the driving force for that deformation. As direct observation and quantification of such
12 aspects is extremely difficult with the techniques and instruments available, simulation
13 studies have been deployed to find the right answers.

14 **Mechanisms revealed by simulations**

15 The simulation models developed so far can be categorized into analytical models and
16 computational (numerical) models. In analytical models, equations based on surface energy
17 considerations, thermodynamic equilibrium and energy minimization are formulated and
18 solved by introducing geometric constraints relating to both the bacteria and the
19 nanostructured surface. The deformation of the adsorbing bacteria, in these models, is
20 considered as a necessity to reach thermodynamic equilibrium. In other words, adsorbing
21 bacteria continue to envelop the nanostructures until equilibrium is reached. These models
22 differ in the way they define the change in free energy (based on local stretching degree and
23 stretching modulus;^{22,25} membrane tension and strain tensors;⁷⁸ work required to bend the
24 bacterial wall around the nanopillar shaft;²⁷ and variation of the adhesion contact angle as the

1 cell migrates into nanopillars²⁸).



2

3 **Figure 7:** a) Forces proposed to drive bacteria towards the nanopillars, b) Energy-based
 4 analytical model of bacterial cell adhering and stretching on nanostructured surfaces in four
 5 configurations depending on the pillar density, the slope and the height. α_A and α_B are the
 6 stretching degrees in regions A and B respectively. The larger stretching degree indicates the
 7 critical action site of that said configuration,^{22,25} c) a contour plot of longitudinal uniaxial
 8 strain for an adhered bacterial envelope. The contact region is probed by L1, the suspended
 9 regions are probed by L2, L3 and L4. At each location, in-plane uniaxial strains are probed at

1 three points through the thickness, representing each of the three layers. For the plasma
2 membrane, the maximal through-thickness value is found at the top plane. For the outer
3 leaflet, the maximal through thickness value is found in the suspended region.⁷⁹ Adapted
4 from ⁷⁹ with permission from Elsevier. Copyright 2021.

5 In computational models, the bacteria-nanostructure interaction is modelled with finite
6 element method based on a major assumption that the bacteria have no fluid surroundings.
7 The simulation models developed so far have thus assumed bacteria-surface interaction in
8 vacuum – an aspect which needs to be evaluated properly. Also, failure of a bacteria is based
9 on the maximum strain in the membrane which is assumed to occur when the local strain
10 value exceeds the permissible strain threshold. The value of this strain threshold reported in
11 the literature shows high percentage variability > 50%, which indicates that the currently
12 reported FEA simulation studies are incoherent. For example, Velic *et al.*⁷⁹ based the rupture
13 strain range on experimentally reported values of the rupture strains of different
14 organisms^{80,81}, bacterial threads⁸², and values obtained from coarse grain modelling of
15 mimetic lipid systems⁸³ (0.18-0.65 as longitudinal strain for the peptidoglycan layer and 0.05-
16 0.35 as areal strain for the outer membrane). Mirzaali *et al.*²³ considered the rupture strain
17 value of 0.5 through the work of Thwaites and Mendelson⁸⁴ which was based on the
18 elongation of *B. subtilis* bacterial thread rather than the elongation of a single bacterium. To
19 add to this dilemma, other studies⁸⁵ have reported vivid values (0.08 for *S. aureus*, 0.12 for *E.*
20 *coli*, and 0.05 for *P. aeruginosa*). Clearly, this important information which is a prerequisite
21 for meaningful finite element simulations needs reinvestigation. The inconsistency reported
22 so far is largely due to the fact that the constitutive modelling of a bacteria is ill-defined and
23 the methods employed to evaluate the mechanical properties of the bacteria were not
24 comprehensive enough. A full set of data can be obtained by fully developing a set of AFM
25 nanoindentation experiments, especially accounting for the anisotropy presented by a

1 bacterium. Clearly one such anomaly which can be seen as an example in the reported
2 literature is the assumption of a gravitational force⁴² acting on the bacteria which is an
3 incorrect assumption since a bacterium is not of its own but is a freely floating particle in a
4 fluid. Therefore, any future modelling studies needs to consider these aspects as well as other
5 aspects, such as the boundary conditions, loading type, strain type etc. very carefully.

6 *The driving forces*

7 To develop any simulation whether analytical or computational, assumptions must be made
8 as to what are the forces driving/governing the phenomenon that is being modelled. Gravity,
9 as shown in Fig. 7 (a), has been incorrectly considered as the main driving force in some
10 studies. Hence, the question arises as to whether the magnitude of a bacterium's gravity is
11 enough to cause its rupture. Xue *et al.*⁴² studied the stretching of bacteria due to gravity on
12 two different geometries: nanopillars and nanoridges. In their model, the stretching degree of
13 the bacterial membrane exceeded the calculated critical stretch value. The rupture of bacterial
14 membrane was inferred to be more likely on nanopillars than nanoridges. Additionally, an
15 FEA study conducted by Velic *et al.*⁸⁶ found that the force of gravity on an *S. aureus*
16 bacterial cell, coupled with the force from the water column above the bacterium (tens of
17 piconewtons) strains it enough, as it contacts a nanostructured surface, to exceed the assumed
18 strain threshold of 0.5. In both studies, the stiffness of the bacterial membrane was assumed
19 to be in the range of a few Pascals to a few kiloPascals (kPa).

20 This is inconsistent with AFM studies which have shown a wide range of stiffness i.e., 0.2 to
21 95 MPa.⁸⁷ Additionally, AFM studies show that bacterial cells including *S. aureus* can
22 withstand forces of several nanoNewtons before its rupture. Based on this, gravity can be
23 ruled out as the main driver for cell rupture.

1 Liu *et al.*²⁸ suggested that cell adsorption is driven by the differential energy gradient (i.e.
2 between Gibbs surface free energy and deformation surface energy) along the height of the
3 nanopillars (i.e. high at the tip of the nanopillar, and low at the base). The force induced by
4 this gradient (100 nN) drives the bacterial cell downwards towards the nanopillars, instigating
5 the elastic deformation of the bacterial cell wall. If pressure or stress exceeds the yield
6 strength of the wall, the latter undergoes creep until rupture. This model can be used to justify
7 the bactericidal effect of a nanostructure on bacteria yet imply a non-cytotoxic effect of such
8 surfaces on mammalian cells. Since the force stems from a differential energy gradient of the
9 nanopillars, the smaller volume of the cell in contact, the larger the effect of the pressure
10 induced on it by a single pillar. It is known that bacterial cells have sizes in the range of few
11 hundreds of nanometers to a few micrometers, whereas mammalian cells are usually in the
12 range of tens to hundreds of micrometers. Thus, according to this model mammalian cells
13 undergo reduced amounts of pressure which do not cause damage to their membranes.

14 Another driving force suggested to cause the rupture of bacteria is the surface energy released
15 as the cell wall binds to the surface.²⁷ If the total surface binding energy is larger than the
16 stretching and bending energy, the bacterial membrane drops below the equilibrium drop
17 height, the tensile stress exceeds the tensile strength of the bacterial membrane, then the
18 membrane tears. In the case of slow binding, influenced by active interactions and responses
19 of the bacteria towards the surface such as hydrophobic interactions, the bacterial death
20 occurs gradually. In the case of fast binding, induced by physical-chemical forces (i.e., van
21 der Waals forces and hydrogen bonding), the rupture occurs instantaneously as the bacterial
22 cell wall binds to the top of the nanopillar with a surplus of energy.

23 Adhesion-driven deformation of the bacterial envelope as it adsorbs onto a nanopillar was
24 also considered in the computational work of Velic *et al.*⁷⁹. In this model, the adhesion was

1 considered as an evolving "bond front" and applied as a downward pressure load on an area
2 that increased in size incrementally.

3 When considering the motility of some bacterial strains or bacteria in flow conditions, the
4 frictional behavior in contact with such surfaces becomes of high importance. Studies report
5 frictional instabilities experienced in contact with nanostructured surfaces where shear tracing
6 showed irregular and sharp peaks across such structured surfaces compared to smooth
7 surfaces⁸⁸. These sharp spikes can present lateral force contributing to the disruptive action of
8 nanoscale features on the bacterial cell wall influencing the bacterial stress response that could
9 manifest in turgor pressure fluctuation and ROS production. The frictional behavior of
10 nanostructured surfaces is highly influenced by the surface specific parameters such as surface
11 roughness parameters⁸⁹, nanofeature geometries, and their densities⁹⁰. In this light, studying
12 nanostructured surfaces exhibiting different frictional behaviors and correlating it with their
13 bactericidal performance, could give new insight into the optimization of the mechano-
14 bactericidal surfaces.

15 *Critical action sites*

16 The competing "penetration" and stretching mechanisms can be considered analogous to the
17 competing critical action sites of a bacterial membrane in analytical and computational
18 modelling. In most energy-based models, the critical action site is in the area suspended
19 between the two pillars^{22,25,45,46,91}. That is because in those models, the bacterial membrane
20 deforms non-uniformly. The stretching of the suspended bacterium occurs to accommodate to
21 the active adsorption onto the nanopillar. Exceptionally, in an extension to work by Pogodin
22 *et al.*,²⁵ Wu *et al.*²² found that by varying the heights of adjacent nanopillars, a higher
23 stretching degree is induced on the membrane region adsorbed onto the nanopillar than on
24 that suspended region. This model is illustrated in Fig. 7 (b). In most computational models,

1 however, the entire membrane undergoes the same force (body force) and the strain across
2 the entire membrane is uniform. The presence of the nanopillars restricts that deformation
3 and induces tension in the membrane at the pillar apex. Interestingly in the computational
4 model that considered adhesion-driven rupture, the critical action sites did not coincide
5 between the layers of the cell wall model of a Gram-negative bacterium (Fig. 7 (c)).
6 Uniquely, the cell wall was modelled as a plasma membrane and peptidoglycan made up of
7 two leaflets. The critical action site for the whole cell envelope was found at the pillar apex as
8 both the inner leaflet and plasma membrane fail at that location with a strain much greater
9 than that transpiring anywhere in the outer leaflet. The critical action site of the outer leaflet
10 of the peptidoglycan, which is in direct contact with the pillar, remains in the suspended
11 region. That is due to the strongly modelled bond between this leaflet’s adsorbed region and
12 the pillar, that forces the reallocation of deformation to the suspended region. Unlike most
13 models, this study did not over-simplify all the complexities of a bacterial membrane and its
14 components nor assumed it to be a planar elastic layer (plane strain). It instead brought
15 attention to (i) the importance of a more detailed multi-layered cell wall model, (ii) the need
16 for three-dimensional analysis of this non-developable problem, and (iii) the significance of
17 force application as a “bond front” mimicking adhesion.

18 In layered bacterial membrane models, as in reality, the stresses that can be withstood by
19 different layers (different materials) vary. In addition, some materials can resist compression
20 more than tension or vice versa. Knowing these material details can help shape the design of
21 the nanostructure to engineer the location of the critical action site appropriately. This can be
22 done by understanding and adjusting the geometrical considerations of nanostructures. It
23 implies the need for developing material constitutive models of bacterial membranes in order
24 to model complex membrane structures reliably.

1 Nevertheless, considering the complexities of the bacteria-nanostructure interaction, factors
2 beyond geometrical considerations can be influential as discussed next.

3 **Factors influencing the bactericidal activity of nanostructured surfaces**

4 The mechano-bactericidal effect is a complex interplay of bacteria and substrate-dependent
5 factors (see Fig. 8), which may be classified into four main categories: geometric, biological,
6 electric and interfacial physical factors.

7 The structural dimensions including the nanofeature radius, shape,
8 interspacing/pitch/nanofeature area density, and height/aspect-ratio are the main constituents
9 of the geometric factor.

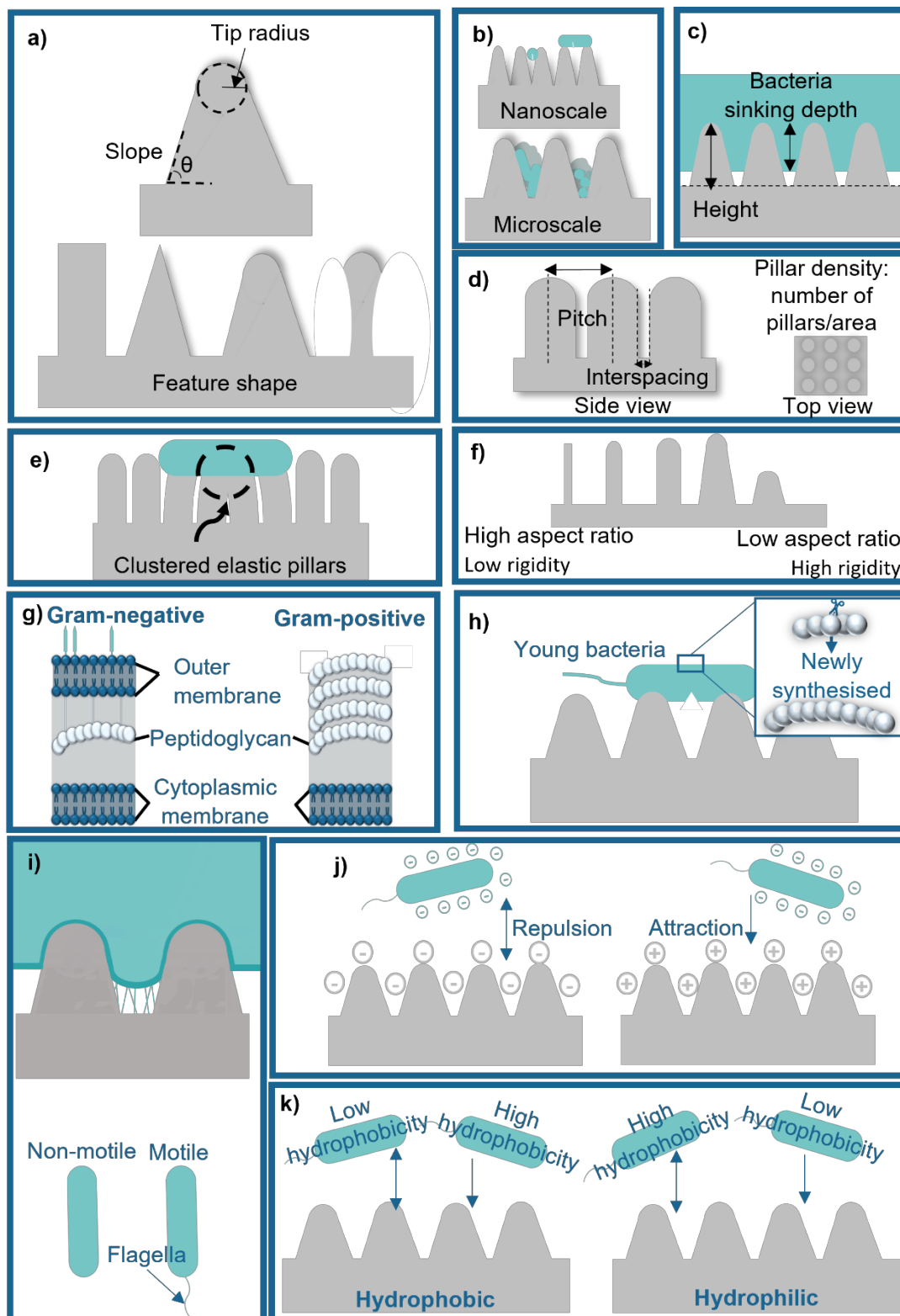
10 *Bacteria-nanofeature contact area: Radius and shape*

11 The tip size of the nanofeature is of great importance because it is the first point of contact
12 between the bacteria and the surface. Studies suggest that a smaller tip radius induces higher
13 pressure on the bacterial membrane and enhances the bactericidal effect of a nanostructured
14 surface.^{14,23,42,92} Some other studies based on the analytical models as previously discussed ,
15 alluded to the fact that a larger radius provides a wider contact area. This pushes the
16 suspended region of the membrane to try and accommodate for the perimeter change by
17 stretching and ultimately rupturing.^{78,79}

18 It is evident that there is a limited range of radii in which nanopillars exhibit enhanced
19 bactericidal effects. According to simulations, that range falls between 50-80 nm,⁴⁶ where the
20 radii is big enough to anchor the bacterial membrane, yet small enough to push bacterial
21 membrane deformation to rupture.

22 The shape of the nanofeatures relates directly to the available contact area (see Fig. 8 (a) and
23 Fig. 9 (A)). Mo *et al.*⁹³ tested micro and nano arrays of cones and pillars and found that

- 1 nanocones, as opposed to pillars, possess enhanced bactericidal activity due to the tip
- 2 sharpness. The slope presented by the nanocone features also plays a role in enhanced
- 3 bactericidal activity as it increases the contact area along the vertical region of the feature.²²



1 **Figure 8:** Factors affecting the efficacy of a mechano-bactericidal surface for a specific
2 bacterial strain. (a) Contact area controlled by feature radius and shape, (b) length scale of the
3 bacteria/structures, (c) height of the structures, (d) the nanofeature interspacing and array
4 density, (e) elasticity of the pillars/structures, (f) aspect ratio-controlled rigidity, (g) Gram
5 stain of the bacteria, (h) age of the bacteria, (i) Surface appendages of the bacteria, (j)
6 electrical charge of the surface and bacteria, (k) the bacteria/surface interfacial-physical
7 factors.

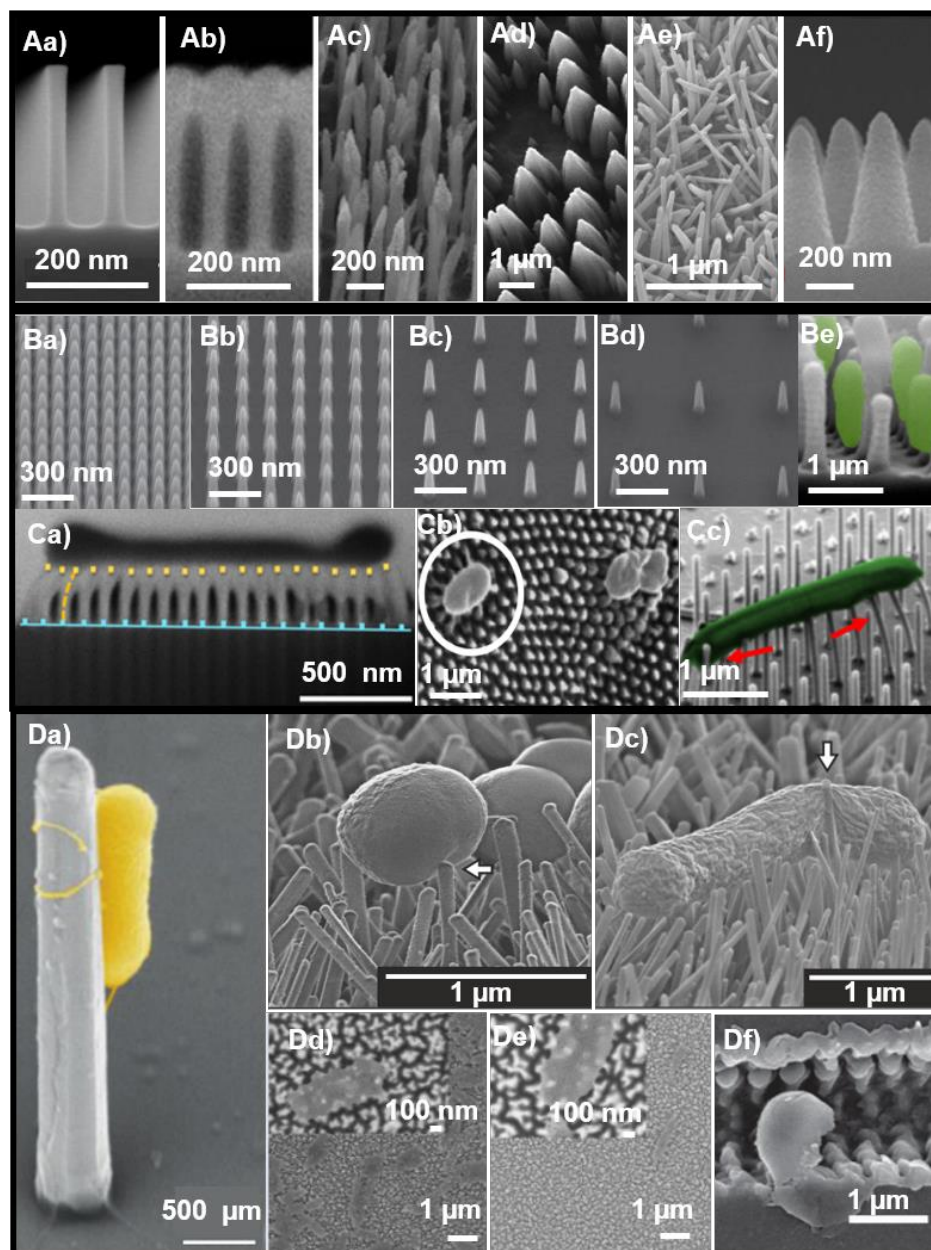
8 *Nanofeature interspacing and array density*

9 For a nanostructured surface to exert stress on a bacterium, the interspacing of the structures
10 needs to be smaller than the diameter of the bacterium, be it cocci or rod-shaped. The
11 bacterium can otherwise align to the spaces between the nanopillars, proliferate and develop a
12 biofilm (see Fig. 8 (b) and Fig. 9 (Be)).⁹⁴ The height of nanopillars should also accommodate
13 the maximum stretching of the bacterial cell wall and be larger than the sinking depth of the
14 bacterium as shown in Fig. 8 (c), otherwise the bacterium will only experience elastic
15 deformation and then rest on the bottom surface with no additional mechanical deformation
16 to cause lysis.

17 Simultaneously, conflicting reports on the role of interspacing in bactericidal efficiency can
18 also be seen. For instance, Mirzaali *et al.*²³ suggested that higher interspacing increases the
19 stretching degree of the bacteria which improves the bactericidal efficiency of the surface but
20 warns that an increased interspacing could lead to cytotoxicity rendering it unsuitable for *in-*
21 *vivo* applications.

22 Their finite element (FE) model predicted a combination of width and interspacing (W= 50
23 nm, IS = 300 nm) to be vital in inducing bactericidal effect against *S. aureus* while avoiding
24 cytotoxic reactions. Conversely, Modaresifar *et al.*³² investigated the effect of interspacing of

1 silicon nanostructures on the viability of *S. aureus* and found that a lower pitch of
 2 interspacing led to an improved bactericidal activity with the highest bactericidal efficiency
 3 achieved for a spacing of 100 nm.



4
 5 Figure 9: **A:** Ranging nanostructure shapes and tip radii; **Aa)** blunt tip nanopillars,⁷⁸ **Ab)**
 6 cotton-swab shaped nanopillars,⁷⁸ **Ac)** sharp nanopillars,¹⁴ **Ad)** sharp conical nanostructures,
 7 reprinted from ref⁴⁷ by permission of AIP Publishing. Copyright 2016, **Ae)** nanowires,³³ **Af)**
 8 cicada-like conical nanostructures, reprinted from ref⁹⁵ by permission of ACS Publications.

1 Copyright 2015. **B:** Ranging interspacing and feature densities;³² **Be)** *P. aeruginosa* aligned
2 between nanopillar interspacing, reprinted from ref⁹⁴ by permission of ACS Publications.
3 Copyright 2010. **C:** Elastic and high aspect ratio structures; **Ca)** enhanced bactericidal effect,
4 reprinted from ref⁹⁶ by permission of PNAS. The yellow dots represent the bacteria-structure
5 interface, blue line represent the alignment of the substrate. **Cb, Cc)** Impeded bactericidal
6 effect. **Cb:** Reprinted from⁹³ by permission of Elsevier. Copyright 2020. **Cc:** Reprinted from
7 ref⁹⁷ by permission of ACS publications. Copyright 2016. **D:** Biological and interfacial
8 physical factors affecting bactericidal efficiency; **Da)** bacterium (i.e. *S. oneidensis*) flagella
9 wrapped around micro-sized pillar to maximize the contact area, reprinted from ref⁹⁸ by
10 permission of ACS Publications. Copyright 2013. **Db)** Gram positive *S. aureus* hardly
11 perturbed on nanowire-like structure,³³ **Dc)** Gram-negative *E. coli* severely deformed on
12 nanowire like structure,³³ **Dd, De)** superhydrophobic structures induce higher hydrophobic-
13 *P. aeruginosa* attachment and death than superhydrophilic structured surface, reprinted from
14 ref¹⁷ by permission of ACS publications. Copyright 2017. **Df)** Positively charged
15 nanostructured surface induces rupture of gram-positive *S. aureus*.⁹⁹

16 Velic *et al.*⁷⁹ agreed that a reduced interspacing increases the bactericidal effect of a
17 nanostructured surface. The authors argued that the simulation studies suggesting the larger
18 interspacing increases the deformation of the envelope had assumed that a "constant" load
19 was being applied. This assumption results in load distribution over a given number of pillars,
20 thus directly inducing more deformation with further spaced pillars and less contact points.
21 On the other hand, in the case of bacterial interaction with nanostructures, the interaction
22 forces are not distributed, but developed at each individual nanopillar.

23 This signifies that more contact points will induce more deformation and a smaller
24 interspacing is bactericidal enhancing.

1 Some studies suggested evaluating the area density of nanofeatures (see Figure 8 (d)) ,
2 instead of their interspacing or pitch, as an important parameter in the adhesion pattern and
3 therefore the stretching degree of the attached bacterial cells.²² Kelleher *et al.*¹⁰⁰ observed a
4 linear correlation between bactericidal activity and the number of nanostructures with which
5 a bacterial cell comes in contact with. In their findings however, the surface that exhibited the
6 highest bactericidal efficiency (and the highest pillar density) was the surface with the highest
7 feature aspect ratio (i.e., ratio of height over width) of around 1.54 with height of 241 nm,
8 pitch 165 nm and diameter 156 nm. In this case, the height and pillar density parameters
9 cannot be decoupled, and the distinction of which parameter had a more significant effect on
10 the bactericidal activity was not possible.

11 *Aspect ratio and rigidity*

12 Few studies have investigated the effect of the aspect ratio and the rigidity of the nanopillars
13 on the bactericidal efficiency of mechano-bactericidal nanostructures. When dealing with
14 elastic pillars, interpillar adhesion and clustering could partially compensate for the force
15 exhibited on the bacterial membrane.^{96,101} This can hinder the bactericidal ability of a surface
16 which is shown in Fig. 8 (e) and Fig. 9 (Cb), however the flexibility of high aspect ratio
17 structures has been shown to enhance elastic energy storage in nanofeatures. They release this
18 energy by bending when in contact with bacteria, which improves the bactericidal activity of
19 the nanostructured surface as shown in Fig. 9 (Ca, Cc).¹⁰² Thus, a threshold exists by which
20 the deformation of the elastic pillar remains favorable to the bactericidal action. The
21 deformation of these nanofeatures is dependent on surface material properties, nanofeature
22 dimensions and the adhesion force of the bacterium to the substratum surface and can be
23 expressed as (in the case of nanopillars) $\Delta x = F_{adhesion} / k$ where k is the pillar stiffness
24 defined as $k = \pi E_{material} \frac{3r^4}{4l^3}$ where r is the radius of the nanopillar and l is its length.

1 As opposed to the elastic modulus of a material, stiffness or eigenvalue of the nanostructure
2 pillar is influenced significantly by its aspect ratio (Fig. 8 (f)). The high aspect ratio
3 nanostructures on the wings of *Palapsalta eyrei* (cicada species) possess an enhanced
4 bactericidal activity and short kill time compared to wings from other cicada species that
5 contain lower aspect ratios, namely *Psaltoda claripennis* and *Aleeta curvicosta*.¹⁰³ The height
6 of the nanofeatures varies from 100 nm to 2 μm , and this largely contributes to the aspect
7 ratio while the diameter is controlled in a limited margin within the fabricated nanopillars.
8 Ivanova *et al.*⁹⁶ reported that a height of 360 nm yielded the most efficient results against
9 both *P. aeruginosa* and *S. aureus* with little to no clustering of the pillars.

10 Generally, the work done in replication and fabrication of mechano-bactericidal structures
11 has failed to report the repeatability in the feature dimensions and geometries which limits
12 direct comparison of results produced by different research groups.¹² However, of the few
13 studies that have successfully reported characterized morphology of the bactericidal surface,
14 the dimensions of effective surfaces were in the range of 100 nm to 1 μm height, 10 to 300
15 nm diameter and less than 500 nm spacing.¹⁰⁴

16 *Biological factors*

17 As the mechano-bactericidal effect is surface and bacteria dependent, it is imperative to pay
18 attention to the biological factors that might influence the bactericidal action observed. These
19 factors, unlike the geometric ones, are not static and most of the time cannot be controlled.

20 For instance, the composition of the bacterial cell wall, as classified by the Gram stain, plays
21 a role in governing its susceptibility to the mechano-bactericidal surfaces. Fig. 8 (g) contrasts
22 the differences between a Gram-positive and Gram-negative bacterial membrane structure.
23 Gram-positive bacteria possess an inner membrane and a thick peptidoglycan layer (20-100
24 nm), whereas Gram-negative bacteria possess outer and inner membranes and an intermediate

1 peptidoglycan layer (only a few nanometers thick).¹⁰⁵ Gram-negative bacteria are thus more
2 susceptible to the killing effect of the nanostructures than Gram-positive bacteria (see Fig. 9
3 (Db, Dc)). Pogodin *et al.*²⁵ found that exposing Gram-positive bacteria (*B. subtilis*,
4 *Planococcus maritimus*, and *S. aureus*) to microwave radiation reduces their rigidity and
5 increases their vulnerability towards the mechano-bactericidal effect of the nanostructured
6 cicada wing surface. In the case of sharp-edged surfaces like black silicon (bSi) with very
7 small tip radii, the sharp edge is able to disrupt both Gram-positive and Gram-negative
8 bacteria leading to their death.¹⁴

9 In addition to the Gram stain, the possession of surface appendages has also been identified
10 as an influencing factor (see Fig. 8 (i)). In a recent study by Ishak *et al.*⁶⁶, bacterial surface
11 proteins have been observed to play a role in facilitating the deformation of the cell wall as
12 represented in Fig. 8 (i) (top). Additionally, the motility and possession of motile appendages
13 (e.g., fully active flagella) has been associated with a higher probability of bacteria being
14 affected by the bactericidal surface¹⁰⁶. Jindai *et al.*³⁵ suggested that since flagella makes the
15 first direct contact with the structured surface, it gets entangled with the surface nanofeatures
16 leaving the bacteria some space to move. The bacteria then suffer abrasions after hitting the
17 surface repeatedly causing effusion of intercellular fluid and death. An SEM micrograph
18 presented in Fig. 9 (Da) shows how the flagellum of a bacterium wraps around a micro-sized
19 pillar.

20 Aside from the Gram stain and motility, a bacterium's membrane will pass in phases of
21 fluctuating rigidity at a young age (< 6 hrs¹⁰⁷) as shown in Fig. 8 (h). This fluctuation occurs
22 when existing peptidoglycan sacculi breaks to incorporate new material and synthesis of a
23 new layer of peptidoglycan is under progress.¹⁰⁷ Thus, younger bacteria are more susceptible
24 to the bactericidal action of nanostructured surfaces than matured bacteria.

1 A few studies have been conducted to test the effect of mechano-bactericidal nanostructures
2 on the adherence and differentiation of eukaryotic human or human-like cells. A common
3 denominator between all these studies is unusual elongated morphology of the cells adhered
4 on these surfaces along with the lack of cellular spreading compared to control smooth
5 surfaces¹⁰⁸. However, Le Clainche *et al.*¹⁰⁹ reported that hASCs were able to proliferate and
6 maintain their ability for trilineage differentiation on such nanostructured surfaces.
7 Additionally, Bhadra *et al.*¹¹⁰ showed that human fibroblasts are able to proliferate and
8 provide a high area coverage on such surfaces. Modaresifar *et al.*¹¹¹ found that the metabolic
9 response of preosteoblast cells was reduced after 14 days on the most efficient bactericidal
10 (40% dead *S. aureus*) surface tested compared to control flat surfaces. Additional
11 standardized studies to study the cytotoxicity of mechano-bactericidal surfaces are needed in
12 order to be able to compare the performance of these surfaces across the board and their
13 applicability to implant surfaces.

14 *Electric and Interfacial-physical*

15 From the mechanisms formerly discussed, the consensus is that mechano-bactericidal activity
16 is a contact phenomenon. Mechano-bactericidal activity can only be invoked by contact,
17 adsorption and adhesion between the bacteria and the surface. The adhesion of the bacteria
18 with the surface is therefore a noteworthy factor in making the surface bactericidal.
19 Adhesion is heavily affected by the electrostatic charge of the bacteria and the substrate and
20 their respective wettability, among other factors (i.e. Lifshitz–Van der Waals forces and
21 Brownian movement forces) as explained by the extended DLVO (XDLVO) theory¹¹².
22 Bacteria are generally negatively charged. If the surface is also negatively charged, repulsion
23 will be dominant (Fig. 8 (j)), and the surface might be called anti-biofouling. For mechano-
24 bactericidal surfaces relying on adhesion to kill bacteria,¹⁰⁴ positive charges can be beneficial

1 as they advocate for the attraction of the bacteria to the surface. Chen *et al.*⁹⁹ combined
2 surface structuring by femtosecond laser and positively charging the surface by Layer-by-
3 Layer (LbL) polyelectrolyte coating in order to enhance the bactericidal effect of the
4 borosilicate glass surface against *S. aureus* and *E. coli* as is presented in Fig. 9 (Df).

5 Generally, the more hydrophobic the bacteria, the higher is its affinity to a hydrophobic
6 surface and greater is the adhesion force between the bacteria and surface as shown in Fig. 8
7 (k) and Fig. 9 (Dd, De). Bacteria of different strains can have differing wettability
8 (hydrophobic or hydrophilic) however, hydrophobicity/hydrophilicity of bacteria can alter
9 depending on the environmental changes and bacterial stage of growth.¹¹³ Both hydrophobic
10 and hydrophilic surfaces can exhibit bactericidal actions against a range of bacterial strains.
11 This leads to the inconclusive role of wettability in the mechanism of mechano-bactericidal
12 action.^{17,114}

13 We must note here that the evaluation of different factors impacting the bactericidal effect of
14 nanostructures was performed either through simulations or experiments. During simulation
15 investigations, the models were based on stretching/penetration mechanisms, which discount
16 the biologically dynamic effects of bacterial cells. In the experiments, the techniques used to
17 evaluate the bactericidal activity of a surface were limited to detection of live/dead bacteria.
18 This limits the understanding of the effect of changing geometrical and electric and
19 interfacial physical factors to how those changes are physically affecting the rupture/death of
20 bacteria. It does not explore the effect of varying those factors on any possible biological
21 mechanism that is leading to bacterial death. In the following section, various experimental
22 techniques that have been used to evaluate bactericidal surfaces and the interaction between
23 bacteria and nanostructured surfaces are further discussed.

1 **Future outlooks**

2 One of the principal challenges that stand in the way of developing and optimizing the
3 mechano-bactericidal surfaces is the ambiguity and uncertainty surrounding the study of their
4 bactericidal mechanism(s).

5 Most evaluation techniques have shown a bias towards specific mechanisms even when
6 seemingly trying to investigate what is behind the killing effect of nanostructured surfaces. It
7 is evident that the influence of engineering in this multidisciplinary problem has long
8 prevailed and the microbiological investigation has not taken its full stride. For engineers and
9 materials scientists, this enigma seems to be solely related to the mechanics of contact and
10 interaction between the nanostructures and the bacteria. That is why the investigations are
11 focused on observing the penetration and deformation of bacteria. These investigations are
12 not of an easy nature because the experimental evaluation and decoupling of the contribution
13 of geometric, electric, and interfacial physical factors are extremely difficult.

14 The problem is even more complex in its essence as it encompasses biological factors.

15 Bacteria are dynamic living cells that behave differently than passive engineering materials.

16 Bacteria can heal small pores induced in their membranes, adjust their turgor pressure to
17 accommodate deformation, induce the production of protective extracellular polymeric
18 matrix under stress, and many other functions that allow them to resist external stressors. This
19 is why it is an opportunistic time for microbiological testing efforts to explore new *in situ*
20 testing methods that can bring us a step further into identifying the reason(s) behind the
21 demise of bacteria in contact with nanostructures at the single cell level, away from bias
22 towards certain proposed mechanisms.

23 Therefore, it is recommended that multiple synchronous and interdisciplinary experimental
24 approaches be employed to avoid experimental bias towards a single mechanism of action
25 and to obtain an affirmative understanding of the mechanism(s) at play for mechano-

1 bactericidal surfaces. Reaching this understanding will allow the combination of different
2 "bactericidal-enhancing" factors to be applied to the design of surfaces targeted to kill
3 common bacteria which are responsible for post-operative infections (i.e., *Staphylococcus*
4 *aureus*, *Coagulase-negative Staphylococcus species*, *Escherichia coli*, *Pseudomonas*
5 *aeruginosa*, *Streptococcus species*), reducing or even eradicating the incidence of deep
6 surgical site infection. As such knowledge is obtained, it is imperative to use similar
7 methodical experimental approaches to understand osteoblast cell interaction with mechano-
8 bactericidal nanostructures to avoid impeding cell bone growth around such surfaces for *in*
9 *vivo* use through biomedical implants. In conjunction with systematic controlled feature
10 design and morphological reporting, this will allow the optimization of the next generation of
11 effective, non-cytotoxic and non-resistant bactericidal surfaces.

12 **Supporting information**

13 The Supporting Information is available free of charge at [link to be inserted].

14 SI 1: Table summarizing the techniques used to evaluate and investigate mechano-bactericidal
15 surfaces to date highlighting their advantages, limitations, and the errors that could possibly occur by
16 their usage.

17 **Author contributions**

18 **Sara Hawi**: Conceptualization, Methodology, Investigation, Resources, Data Curation,
19 Writing-original draft, **Saurav Goel**: Methodology, Resources, reviewing and editing,
20 Supervision, Project administration, Funding acquisition. **Vinod Kumar**: Writing-reviewing
21 and editing, Supervision. **Oliver Pearce, Wayne Nishio Ayre and Elena P. Ivanova**:
22 Experimental support, Knowledge sharing, Improvement in the draft and reviewing

23 **Data statement**

24 As this is a review paper, no new data was generated.

1 **Acknowledgements**

2 All authors tremendously appreciate and acknowledge the Vice-Chancellor Fellowship of
3 Cranfield University to support SH's PhD study. The financial support provided by the UKRI
4 via Grants No. EP/L016567/1, EP/S013652/1, EP/S036180/1, EP/T001100/1 and
5 EP/T024607/1, TFIN+ Feasibility study award to LSBU (EP/V026402/1), the Royal
6 Academy of Engineering via Grants No. IAPP18-19\295 and TSP1332, EURAMET EMPIR
7 A185 (2018) and the Newton Fellowship award from the Royal Society (NIF\R1\191571) is
8 greatly acknowledged. Wherever applicable, the work made use of Isambard Bristol, UK
9 supercomputing service accessed by a Resource Allocation Panel (RAP) grant as well as
10 ARCHER resources (Project e648).

11

12 **Notes**

13 The authors declare no competing financial interest.

14

15 **Vocabulary**

16 **Mechano-bactericidal**, a functionality of a structure to kill bacteria mechanically without the
17 need for chemical intervention. **Peptidoglycan**, a mesh-like polymeric structural element of
18 the bacterial cell wall. It consists of glycan strands cross-linked by short peptides which form
19 a closed structure bordering the cytoplasmic membrane of the bacterium. The peptidoglycan
20 layer is substantially thicker for Gram-positive bacteria than Gram-negative. **Cytotoxicity**, a
21 term used to describe a surface, substance or process that causes cell damage and death. In the
22 context of this paper, it is used to describe undesired human cell damage. **Incubation**, the
23 process of culturing bacteria under specific conditions that are optimal for their growth. That

1 includes a controlled temperature and access to bacteria-specific nutrients. **In vivo**, a
2 process/experiment that takes in a living organism e.g., mechano-bactericidal implant
3 implanted in animals. **Adsorption**, a substance is said to be adsorbed when it is concentrated
4 reversibly at a surface. Here, physical adsorption or physisorption is being referred to where
5 the main interacting force is Van der Waals which, along with other interactions (Fig. 6 (a)),
6 influences the initial bacterial attachment to the surface. **Strain**, it represents elongation or
7 shortening in dimension in response to an applied force in the Mechanical Engineering
8 discipline but in biological discipline it is also used to distinguish subtype of a
9 microorganism (e.g., a virus, bacterium, or fungus)

10 **References**

- 11 (1) Goel, S.; Hawi, S.; Goel, G.; Thakur, V. K.; Agrawal, A.; Hoskins, C.; Pearce, O.;
12 Hussain, T.; Upadhyaya, H. M.; Cross, G.; Barber, A. H. Resilient and Agile
13 Engineering Solutions to Address Societal Challenges Such as Coronavirus Pandemic.
14 *Mater. Today Chem.* **2020**, *17*. <https://doi.org/10.1016/j.mtchem.2020.100300>.
- 15 (2) Spellberg, B.; Gilbert, D. N. The Future of Antibiotics and Resistance: A Tribute to a
16 Career of Leadership by John Bartlett. *Clin. Infect. Dis.* **2014**, *59* (Suppl 2), S71–S75.
17 <https://doi.org/10.1093/cid/ciu392>.
- 18 (3) Pham, V. T. H.; Truong, V. K.; Orłowska, A.; Ghanaati, S.; Barbeck, M.; Booms, P.;
19 Fulcher, A. J.; Bhadra, C. M.; Buividas, R.; Baulin, V.; James Kirkpatrick, C.; Doran,
20 P.; Mainwaring, D. E.; Juodkasis, S.; Crawford, R. J.; Ivanova, E. P. Race for the
21 Surface: Eukaryotic Cells Can Win. *ACS Appl. Mater. Interfaces* **2016**, *8* (34), 22025–
22 22031. <https://doi.org/10.1021/acsami.6b06415>.
- 23 (4) Bauer, T. W.; Schils, J. The Pathology of Total Joint Arthroplasty. I. Mechanisms of
24 Implant Fixation. *Skeletal Radiol.* **1999**, *28* (9), 483–497.

- 1 <https://doi.org/10.1007/s002560050552>.
- 2 (5) Zimmerli, W.; Trampuz, A.; Ochsner, P. E. Prosthetic-Joint Infections. **2004**, 1645–
3 1654.
- 4 (6) Kümin, M.; Harper, C. M.; Reed, M.; Bremner, S.; Perry, N.; Scarborough, M.
5 Reducing Implant Infection in Orthopaedics (RIiO): A Pilot Study for a Randomised
6 Controlled Trial Comparing the Influence of Forced Air versus Resistive Fabric
7 Warming Technologies on Postoperative Infection Rates Following Orthopaedic
8 Implant Surgery I. *Trials* **2018**, *19* (1), 1–8. [https://doi.org/10.1186/s13063-018-3011-](https://doi.org/10.1186/s13063-018-3011-y)
9 [y](https://doi.org/10.1186/s13063-018-3011-y).
- 10 (7) Moriarty, T. F.; Kuehl, R.; Coenye, T.; Metsemakers, W. J.; Morgenstern, M.;
11 Schwarz, E. M.; Riool, M.; Zaat, S. A. J.; Khana, N.; Kates, S. L.; Geoff Richards, R.
12 Orthopaedic Device-Related Infection: Current and Future Interventions for Improved
13 Prevention and Treatment. *EFORT Open Rev.* **2016**, *1* (4), 89–99.
14 <https://doi.org/10.1302/2058-5241.1.000037>.
- 15 (8) Microbiology Services. *UK Standards for Microbiology Investigations Investigation of*
16 *Orthopaedic Implant Associated Infections*; 2016; Vol. B44.
- 17 (9) Stogios, P. J.; Savchenko, A. Molecular Mechanisms of Vancomycin Resistance.
18 *Protein Sci.* **2020**, *29* (3), 654–669. <https://doi.org/10.1002/pro.3819>.
- 19 (10) Fernández, L.; Gooderham, W. J.; Bains, M.; McPhee, J. B.; Wiegand, I.; Hancock, R.
20 E. W. Adaptive Resistance to the “Last Hope” Antibiotics Polymyxin B and Colistin in
21 *Pseudomonas Aeruginosa* Is Mediated by the Novel Two-Component Regulatory
22 System ParR-ParS. *Antimicrob. Agents Chemother.* **2010**, *54* (8), 3372–3382.
23 <https://doi.org/10.1128/AAC.00242-10>.

- 1 (11) Vimbela, G. V.; Ngo, S. M.; Fraze, C.; Yang, L.; Stout, D. A. Antibacterial Properties
2 and Toxicity from Metallic Nanomaterials. *Int. J. Nanomedicine* **2017**, *12*, 3941–3965.
3 <https://doi.org/10.2147/IJN.S134526>.
- 4 (12) Lin, N.; Berton, P.; Moraes, C.; Rogers, R. D.; Tufenkji, N. Nanodarts, Nanoblades,
5 and Nanospikes: Mechano-Bactericidal Nanostructures and Where to Find Them. *Adv.*
6 *Colloid Interface Sci.* **2018**, *252*, 55–68. <https://doi.org/10.1016/j.cis.2017.12.007>.
- 7 (13) Ivanova, E. P.; Hasan, J.; Webb, H. K.; Truong, V. K.; Watson, G. S.; Watson, J. A.;
8 Baulin, V. A.; Pogodin, S.; Wang, J. Y.; Tobin, M. J.; Löbbe, C.; Crawford, R. J.
9 Natural Bactericidal Surfaces: Mechanical Rupture of Pseudomonas Aeruginosa Cells
10 by Cicada Wings. *Small* **2012**, *8* (16), 2489–2494.
11 <https://doi.org/10.1002/sml.201200528>.
- 12 (14) Ivanova, E. P.; Hasan, J.; Webb, H. K.; Gervinskas, G.; Juodkazis, S.; Truong, V. K.;
13 Wu, A. H. F.; Lamb, R. N.; Baulin, V. A.; Watson, G. S.; Watson, J. A.; Mainwaring,
14 D. E.; Crawford, R. J. Bactericidal Activity of Black Silicon. *Nat. Commun.* **2013**, 1–7.
15 <https://doi.org/10.1038/ncomms3838>.
- 16 (15) Li, Q. A Practical Fabrication Method of the Gecko-Inspired Easy-Removal Skin
17 Adhesives. *Biosurface and Biotribology* **2017**, *3* (2), 66–74.
18 <https://doi.org/10.1016/j.bsbt.2017.06.003>.
- 19 (16) Bandara, C. D.; Singh, S.; Afara, I. O.; Wolff, A.; Tesfamichael, T.; Ostrikov, K.;
20 Oloyede, A. Bactericidal Effects of Natural Nanotopography of Dragonfly Wing on
21 Escherichia Coli. *ACS Appl. Mater. Interfaces* **2017**, *9* (8), 6746–6760.
22 <https://doi.org/10.1021/acsami.6b13666>.
- 23 (17) Linklater, D. P.; Juodkazis, S.; Rubanov, S.; Ivanova, E. P. Comment on “Bactericidal
24 Effects of Natural Nanotopography of Dragonfly Wing on Escherichia Coli.” *ACS*

- 1 *Appl. Mater. Interfaces* **2017**, 9 (35), 29387–29393.
2 <https://doi.org/10.1021/acsami.7b05707>.
- 3 (18) Tripathy, A.; Sen, P.; Su, B.; Briscoe, W. H. Natural and Bioinspired Nanostructured
4 Bactericidal Surfaces. *Adv. Colloid Interface Sci.* **2017**, 248, 85–104.
5 <https://doi.org/10.1016/j.cis.2017.07.030>.
- 6 (19) Linklater, D. P.; Juodkazis, S.; Ivanova, E. P. Nanofabrication of Mechano-
7 Bactericidal Surfaces. *Nanoscale* **2017**, 9 (43), 16564–16585.
8 <https://doi.org/10.1039/c7nr05881k>.
- 9 (20) Elbourne, A.; Crawford, R. J.; Ivanova, E. P. Nano-Structured Antimicrobial Surfaces:
10 From Nature to Synthetic Analogues. *J. Colloid Interface Sci.* **2017**, 508 (January
11 2018), 603–616. <https://doi.org/10.1016/j.jcis.2017.07.021>.
- 12 (21) Jaggessar, A.; Shahali, H.; Mathew, A.; Yarlagaadda, P. K. D. V. Bio-Mimicking Nano
13 and Micro-Structured Surface Fabrication for Antibacterial Properties in Medical
14 Implants. *J. Nanobiotechnology* **2017**, 15 (1), 1–20. [https://doi.org/10.1186/s12951-](https://doi.org/10.1186/s12951-017-0306-1)
15 [017-0306-1](https://doi.org/10.1186/s12951-017-0306-1).
- 16 (22) Wu, S.; Zuber, F.; Maniura-Weber, K.; Brugger, J.; Ren, Q. Nanostructured Surface
17 Topographies Have an Effect on Bactericidal Activity. *J. Nanobiotechnology* **2018**, 16
18 (1), 1–9. <https://doi.org/10.1186/s12951-018-0347-0>.
- 19 (23) Mirzaali, M. J.; Van Dongen, I. C. P.; Tümer, N.; Weinans, H.; Amin Yavari, S.;
20 Zadpoor, A. A. In-Silico Quest for Bactericidal but Non-Cytotoxic Nanopatterns.
21 *Nanotechnology* **2018**, 29 (43). <https://doi.org/10.1088/1361-6528/aad9bf>.
- 22 (24) Luan, Y.; Liu, S.; Pihl, M.; Mei, H. C. Van Der; Liu, J.; Hizal, F.; Choi, C.; Chen, H.;
23 Ren, Y.; Busscher, H. J. Bacterial Interactions with Nanostructured Surfaces. *Curr.*

- 1 *Opin. Colloid Interface Sci.* **2018**, 38, 170–189.
2 <https://doi.org/10.1016/j.cocis.2018.10.007>.
- 3 (25) Pogodin, S.; Hasan, J.; Baulin, V. A.; Webb, H. K.; Truong, V. K.; Phong Nguyen, T.
4 H.; Boshkovikj, V.; Fluke, C. J.; Watson, G. S.; Watson, J. A.; Crawford, R. J.;
5 Ivanova, E. P. Biophysical Model of Bacterial Cell Interactions with Nanopatterned
6 Cicada Wing Surfaces. *Biophys. J.* **2013**, 104 (4), 835–840.
7 <https://doi.org/10.1016/j.bpj.2012.12.046>.
- 8 (26) Hazell, G.; Fisher, L. E.; Murray, W. A.; Nobbs, A. H.; Su, B. Bioinspired Bactericidal
9 Surfaces with Polymer Nanocone Arrays. *J. Colloid Interface Sci.* **2018**, 528, 389–399.
10 <https://doi.org/10.1016/j.jcis.2018.05.096>.
- 11 (27) Watson, G. S.; Green, D. W.; Watson, J. A.; Zhou, Z.; Li, X.; Cheung, G. S. P.;
12 Gellender, M. A Simple Model for Binding and Rupture of Bacterial Cells on
13 Nanopillar Surfaces. *Adv. Mater. Interfaces* **2019**, 6 (10), 1–8.
14 <https://doi.org/10.1002/admi.201801646>.
- 15 (28) Liu, T.; Cui, Q.; Wu, Q.; Li, X.; Song, K.; Ge, D.; Guan, S. Mechanism Study of
16 Bacteria Killed on Nanostructures. *J. Phys. Chem. B* **2019**, 123 (41), 8686–8696.
17 <https://doi.org/10.1021/acs.jpcc.9b07732>.
- 18 (29) Elbourne, A.; Chapman, J.; Gelmi, A.; Cozzolino, D.; Crawford, R. J.; Truong, V. K.
19 Bacterial-Nanostructure Interactions: The Role of Cell Elasticity and Adhesion Forces.
20 *J. Colloid Interface Sci.* **2019**, 546, 192–210.
21 <https://doi.org/10.1016/j.jcis.2019.03.050>.
- 22 (30) Dunseath, O.; Smith, E. J. W.; Al-Jeda, T.; Smith, J. A.; King, S.; May, P. W.; Nobbs,
23 A. H.; Hazell, G.; Welch, C. C.; Su, B. Studies of Black Diamond as an Antibacterial
24 Surface for Gram Negative Bacteria: The Interplay between Chemical and Mechanical

- 1 Bactericidal Activity. *Sci. Rep.* **2019**, *9* (1), 1–10. [https://doi.org/10.1038/s41598-019-](https://doi.org/10.1038/s41598-019-45280-2)
2 45280-2.
- 3 (31) Nguyen, D. H. K.; Loebbe, C.; Linklater, D. P.; Xu, X.; Vrancken, N.; Katkus, T.;
4 Juodkazis, S.; Maclaughlin, S.; Baulin, V.; Crawford, R. J.; Ivanova, E. P. The
5 Idiosyncratic Self-Cleaning Cycle of Bacteria on Regularly Arrayed Mechano-
6 Bactericidal Nanostructures. *Nanoscale* **2019**, *11* (35), 16455–16462.
7 <https://doi.org/10.1039/c9nr05923g>.
- 8 (32) Modaresifar, K.; Kunkels, L. B.; Ganjian, M.; Tümer, N.; Hagen, C. W.; Otten, L. G.;
9 Hagedoorn, P. L.; Angeloni, L.; Ghatkesar, M. K.; Fratila-Apachitei, L. E.; Zadpoor,
10 A. A. Deciphering the Roles of Interspace and Controlled Disorder in the Bactericidal
11 Properties of Nanopatterns against *Staphylococcus Aureus*. *Nanomaterials* **2020**, *10*
12 (2). <https://doi.org/10.3390/nano10020347>.
- 13 (33) Jenkins, J.; Mantell, J.; Neal, C.; Gholinia, A.; Verkade, P.; Nobbs, A. H.; Su, B.
14 Antibacterial Effects of Nanopillar Surfaces Are Mediated by Cell Impedance,
15 Penetration and Induction of Oxidative Stress. *Nat. Commun.* **2020**, *11* (1).
16 <https://doi.org/10.1038/s41467-020-15471-x>.
- 17 (34) Valiei, A.; Lin, N.; Bryche, J.-F.; McKay, G.; Canva, M.; Charette, P. G.; Nguyen, D.;
18 Moraes, C.; Tufenkji, N. Hydrophilic Mechano-Bactericidal Nanopillars Require
19 External Forces to Effectively Kill Bacteria. **2020**, 1–22.
- 20 (35) Jindai, K.; Nakade, K.; Masuda, K.; Sagawa, T.; Kojima, H.; Shimizu, T.; Shingubara,
21 S.; Ito, T. Adhesion and Bactericidal Properties of Nanostructured Surfaces Dependent
22 on Bacterial Motility. *RSC Adv.* **2020**, *10* (10), 5673–5680.
23 <https://doi.org/10.1039/c9ra08282d>.
- 24 (36) Pham, V. T. H.; Truong, V. K.; Mainwaring, D. E.; Guo, Y.; Baulin, V. A.; Al

- 1 Kobaisi, M.; Gervinskas, G.; Juodkazis, S.; Zeng, W. R.; Doran, P. P.; Crawford, R. J.;
2 Ivanova, E. P. Nanotopography as a Trigger for the Microscale, Autogenous and
3 Passive Lysis of Erythrocytes. *J. Mater. Chem. B* **2014**, *2* (19), 2819–2826.
4 <https://doi.org/10.1039/c4tb00239c>.
- 5 (37) Kamarajan, B. P.; Muthusamy, A. Survival Strategy of *Pseudomonas Aeruginosa* on
6 the Nanopillar Topography of Dragonfly (*Pantala Flavescens*) Wing. *AMB Express*
7 **2020**, *10* (1). <https://doi.org/10.1186/s13568-020-01021-7>.
- 8 (38) Linklater, D. P.; Baulin, V. A.; Juodkazis, S.; Crawford, R. J.; Stoodley, P.; Ivanova,
9 E. P. Mechano-Bactericidal Actions of Nanostructured Surfaces. *Nat. Rev. Microbiol.*
10 **2020**, 9–12. <https://doi.org/10.1038/s41579-020-0414-z>.
- 11 (39) Larrañaga-altuna, M.; Zabala, A.; Llavori, I.; Pearce, O.; Dinh, T. Bactericidal
12 Surfaces : An Emerging 21st Century Ultra-Precision Manufacturing and Materials
13 Puzzle. *Appl. Phys. Rev.* **2020**, No. December, 1–75.
14 <https://doi.org/10.1063/5.0028844>.
- 15 (40) Roy, A.; Chatterjee, K. Theoretical and Computational Investigations into
16 Mechanobactericidal Activity of Nanostructures at the Bacteria-Biomaterial Interface:
17 A Critical Review. *Nanoscale* **2021**, *13* (2), 647–658.
18 <https://doi.org/10.1039/d0nr07976f>.
- 19 (41) Senevirathne, S. W. M. A. I.; Hasan, J.; Mathew, A.; Woodruff, M.; Yarlagadda, P. K.
20 D. V. Bactericidal Efficiency of Micro- And Nanostructured Surfaces: A Critical
21 Perspective. *RSC Adv.* **2021**, *11* (3), 1883–1900. <https://doi.org/10.1039/d0ra08878a>.
- 22 (42) Xue, F.; Liu, J.; Guo, L.; Zhang, L.; Li, Q. Theoretical Study on the Bactericidal
23 Nature of Nanopatterned Surfaces. *J. Theor. Biol.* **2015**, *385*, 1–7.
24 <https://doi.org/10.1016/j.jtbi.2015.08.011>.

- 1 (43) Watson, G. S.; Green, D. W.; Schwarzkopf, L.; Li, X.; Cribb, B. W.; Myhra, S.;
2 Watson, J. A. A Gecko Skin Micro/Nano Structure - A Low Adhesion,
3 Superhydrophobic, Anti-Wetting, Self-Cleaning, Biocompatible, Antibacterial Surface.
4 *Acta Biomater.* **2015**, *21*, 109–122. <https://doi.org/10.1016/j.actbio.2015.03.007>.
- 5 (44) Bhadra, C. M.; Khanh Truong, V.; Pham, V. T. H.; Al Kobaisi, M.; Seniutinas, G.;
6 Wang, J. Y.; Juodkazis, S.; Crawford, R. J.; Ivanova, E. P. Antibacterial Titanium
7 Nano-Patterned Arrays Inspired by Dragonfly Wings. *Sci. Rep.* **2015**, *5*, 1–12.
8 <https://doi.org/10.1038/srep16817>.
- 9 (45) Li, X. Bactericidal Mechanism of Nanopatterned Surfaces. *Phys. Chem. Chem. Phys.*
10 **2016**, *18* (2), 1311–1316. <https://doi.org/10.1039/c5cp05646b>.
- 11 (46) Li, X.; Chen, T. Enhancement and Suppression Effects of a Nanopatterned Surface on
12 Bacterial Adhesion. **2016**, *052419*, 1–7. <https://doi.org/10.1103/PhysRevE.93.052419>.
- 13 (47) Fisher, L. E.; Yang, Y.; Hobbs, A.; Yuen, M.-F.; Zhang, W.; Su, B. Bactericidal
14 Activity of Biomimetic Diamond Nanocone Surfaces. *J. Biomater. Biol. Interfaces*
15 **2016**.
- 16 (48) Ivanova, E. P.; Hasan, J.; Webb, H. K.; Truong, V. K.; Watson, G. S.; Watson, J. A.;
17 Baulin, V. A.; Pogodin, S.; Wang, J. Y.; Tobin, M. J.; Löbbecke, C.; Crawford, R. J.
18 Natural Bactericidal Surfaces: Mechanical Rupture of *Pseudomonas Aeruginosa* Cells
19 by Cicada Wings. *Small* **2012**, *8* (16), 2489–2494.
20 <https://doi.org/10.1002/sml.201200528>.
- 21 (49) Hasan, J.; Pyke, A.; Nair, N.; Yarlagadda, T.; Will, G.; Spann, K.; Yarlagadda, P. K.
22 D. V. Antiviral Nanostructured Surfaces Reduce the Viability of SARS-CoV-2. *ACS*
23 *Biomater. Sci. Eng.* **2020**, *6* (9), 4858–4861.
24 <https://doi.org/10.1021/acsbio.2020.001091>.

- 1 (50) Nowlin, K.; Boseman, A.; Covell, A.; LaJeunesse, D. Adhesion-Dependent Rupturing
2 of *Saccharomyces Cerevisiae* on Biological Antimicrobial Nanostructured Surfaces. *J.*
3 *R. Soc. Interface* **2014**, *12* (102). <https://doi.org/10.1098/rsif.2014.0999>.
- 4 (51) Parry, B. R.; Surovtsev, I. V.; Cabeen, M. T.; O'Hern, C. S.; Dufresne, E. R.; Jacobs-
5 Wagner, C. The Bacterial Cytoplasm Has Glass-like Properties and Is Fluidized by
6 Metabolic Activity. *Cell* **2014**, *156* (0), 183–194.
7 <https://doi.org/doi:10.1016/j.cell.2013.11.028>.
- 8 (52) Wolf, A. J.; Underhill, D. M. Peptidoglycan Recognition by the Innate Immune
9 System. *Nat. Rev. Immunol.* **2018**, *18* (4), 243–254.
10 <https://doi.org/10.1038/nri.2017.136>.
- 11 (53) Vadillo-Rodriguez, V.; Beveridge, T. J.; Dutcher, J. R. Surface Viscoelasticity of
12 Individual Gram-Negative Bacterial Cells Measured Using Atomic Force Microscopy.
13 *J. Bacteriol.* **2008**, *190* (12), 4225–4232. <https://doi.org/10.1128/JB.00132-08>.
- 14 (54) Dimova, R. Recent Developments in the Field of Bending Rigidity Measurements on
15 Membranes. *Adv. Colloid Interface Sci.* **2014**, *208*, 225–234.
16 <https://doi.org/10.1016/j.cis.2014.03.003>.
- 17 (55) Trapalis, C. C.; Keivanidis, P.; Kordas, G.; Zaharescu, M.; Crisan, M.; Szatvanyi, A.;
18 Gartner, M. TiO₂(Fe³⁺) Nanostructured Thin Films with Antibacterial Properties.
19 *Thin Solid Films* **2003**, *433* (1-2 SPEC.), 186–190. <https://doi.org/10.1016/S0040->
20 [6090\(03\)00331-6](https://doi.org/10.1016/S0040-6090(03)00331-6).
- 21 (56) Rajab, F. H.; Liauw, C. M.; Benson, P. S.; Li, L.; Whitehead, K. A. Picosecond Laser
22 Treatment Production of Hierarchical Structured Stainless Steel to Reduce Bacterial
23 Fouling. *Food Bioprod. Process.* **2018**, *109*, 29–40.
24 <https://doi.org/10.1016/j.fbp.2018.02.009>.

- 1 (57) Lutey, A. H. A.; Gemini, L.; Romoli, L.; Lazzini, G.; Fuso, F.; Faucon, M.; Kling, R.
2 Towards Laser-Textured Antibacterial Surfaces. *Sci. Rep.* **2018**, *8* (1), 1–10.
3 <https://doi.org/10.1038/s41598-018-28454-2>.
- 4 (58) Valiei, A.; Lin, N.; Bryche, J.; Canva, M.; Charette, P. G.; Nguyen, D.; Moraes, C.;
5 Tufenkji, N. Hydrophilic Mechano-Bactericidal Nanopillars Require External Forces
6 to Rapidly Kill Bacteria. *ACS Nanolett* **2020**.
7 <https://doi.org/10.1021/acs.nanolett.0c01343>.
- 8 (59) Cerca, N.; Pier, G. B.; Vilanova, M.; Oliveira, R.; Azeredo, J. Quantitative Analysis of
9 Adhesion and Biofilm Formation on Hydrophilic and Hydrophobic Surfaces of
10 Clinical Isolates of Staphylococcus Epidermidis. *Res. Microbiol.* **2008**, *23* (1), 1–7.
- 11 (60) Sieradzki, K.; Tomasz, A. Alterations of Cell Wall Structure and Metabolism
12 Accompany Reduced Susceptibility to Vancomycin in an Isogenic Series of Clinical
13 Isolates of Staphylococcus Aureus. *J. Bacteriol.* **2003**, *185* (24), 7103–7110.
14 <https://doi.org/10.1128/JB.185.24.7103-7110.2003>.
- 15 (61) Olsson, A. L. J.; Sharma, P. K.; van der Mei, H. C.; Busscher, H. J. Adhesive Bond
16 Stiffness of Staphylococcus Aureus with and without Proteins That Bind to an
17 Adsorbed Fibronectin Film. *Appl. Environ. Microbiol.* **2012**, *78* (1), 99–102.
18 <https://doi.org/10.1128/AEM.06912-11>.
- 19 (62) Foster, T. J.; Geoghegan, J. A.; Ganesh, V. K.; Höök, M. Adhesion, Invasion and
20 Evasion: The Many Functions of the Surface Proteins of Staphylococcus Aureus. *Nat.*
21 *Rev. Microbiol.* **2014**, *12* (1), 49–62. <https://doi.org/10.1038/nrmicro3161>.
- 22 (63) Michalska, M.; Divan, R.; Noirot, P.; Laible, P. D. Antimicrobial Properties of
23 Nanostructured Surfaces – Demonstrating the Need for a Standard Testing
24 Methodology. *Nanoscale* **2021**, *13* (41), 17603–17614.

- 1 <https://doi.org/10.1039/d1nr02953c>.
- 2 (64) Rhee, K. Y.; Gardiner, D. F. Clinical Relevance of Bacteriostatic versus Bactericidal
3 Activity in the Treatment of Gram-Positive Bacterial Infections [2]. *Clin. Infect. Dis.*
4 **2004**, *39* (5), 755–756. <https://doi.org/10.1086/422881>.
- 5 (65) Chopinet, L.; Formosa, C.; Rols, M. P.; Duval, R. E.; Dague, E. Imaging Living Cells
6 Surface and Quantifying Its Properties at High Resolution Using AFM in QI™ Mode.
7 *Micron* **2013**, *48*, 26–33. <https://doi.org/10.1016/j.micron.2013.02.003>.
- 8 (66) Ishak, M. I.; Jenkins, J.; Kulkarni, S.; Keller, T. F.; Briscoe, W. H.; Nobbs, A. H.; Su,
9 B. Insights into Complex Nanopillar-Bacteria Interactions: Roles of Nanotopography
10 and Bacterial Surface Proteins. *J. Colloid Interface Sci.* **2021**, *604*, 91–103.
11 <https://doi.org/10.1016/j.jcis.2021.06.173>.
- 12 (67) Bailey, R. G.; Turner, R. D.; Mullin, N.; Clarke, N.; Foster, S. J.; Hobbs, J. K. The
13 Interplay between Cell Wall Mechanical Properties and the Cell Cycle in
14 Staphylococcus Aureus. *Biophys. J.* **2014**, *107* (11), 2538–2545.
15 <https://doi.org/10.1016/j.bpj.2014.10.036>.
- 16 (68) Dorobantu, L. S.; Gray, M. R. Application of Atomic Force Microscopy in Bacterial
17 Research. *Scanning* **2010**, *32* (2), 74–96. <https://doi.org/10.1002/sca.20177>.
- 18 (69) Hizal, F.; Choi, C. H.; Busscher, H. J.; Van Der Mei, H. C. Staphylococcal Adhesion,
19 Detachment and Transmission on Nanopillared Si Surfaces. *ACS Appl. Mater.*
20 *Interfaces* **2016**, *8* (44), 30430–30439. <https://doi.org/10.1021/acsami.6b09437>.
- 21 (70) Li, L.; Tian, F.; Chang, H.; Zhang, J.; Wang, C.; Rao, W.; Hu, H. Interactions of
22 Bacteria With Monolithic Lateral Silicon Nanospikes Inside a Microfluidic Channel.
23 *Front. Chem.* **2019**, *7* (July), 1–8. <https://doi.org/10.3389/fchem.2019.00483>.

- 1 (71) Kamarajan, B. P.; Ananthasubramanian, M.; Sriramajayam, L.; Boppe, A. Behavior of
2 Pseudomonas Aeruginosa Strains on the Nanopillar Topography of Dragonfly (
3 Pantala Flavescens) Wing under Flow Conditions . *Biointerphases* **2021**, *16* (5),
4 051002. <https://doi.org/10.1116/6.0001303>.
- 5 (72) Jenkins, J.; Ishak, M. I.; Eales, M.; Gholinia, A.; Kulkarni, S.; Keller, T. F.; May, P.
6 W.; Nobbs, A. H.; Su, B. Resolving Physical Interactions between Bacteria and
7 Nanotopographies with Focused Ion Beam Scanning Electron Microscopy. *iScience*
8 **2021**, *24* (7). <https://doi.org/10.1016/j.isci.2021.102818>.
- 9 (73) Nakade, K.; Jindai, K.; Sagawa, T.; Kojima, H.; Shimizu, T.; Shingubara, S.; Ito, T.
10 Single Cell / Real-Time Imaging of Bactericidal Effect on the Nanostructural Surface.
11 *Mater. Today Proc.* **2019**, *7*, 497–500. <https://doi.org/10.1016/j.matpr.2018.11.115>.
- 12 (74) Cheng, Y.; Feng, G.; Moraru, C. I. Micro-and Nanotopography Sensitive Bacterial
13 Attachment Mechanisms: A Review. *Front. Microbiol.* **2019**, *10* (FEB), 1–17.
14 <https://doi.org/10.3389/fmicb.2019.00191>.
- 15 (75) Hasan, J.; Webb, H. K.; Truong, V. K.; Pogodin, S.; Baulin, V. A.; Watson, G. S.;
16 Watson, J. A.; Crawford, R. J.; Ivanova, E. P. Selective Bactericidal Activity of
17 Nanopatterned Superhydrophobic Cicada Psaltoda Claripennis Wing Surfaces. *Appl.*
18 *Microbiol. Biotechnol.* **2013**, *97* (20), 9257–9262. [https://doi.org/10.1007/s00253-012-](https://doi.org/10.1007/s00253-012-4628-5)
19 [4628-5](https://doi.org/10.1007/s00253-012-4628-5).
- 20 (76) Hong, Y.; Zeng, J.; Wang, X.; Drlica, K.; Zhao, X. Post-Stress Bacterial Cell Death
21 Mediated by Reactive Oxygen Species. *Proc. Natl. Acad. Sci. U. S. A.* **2019**, *116* (20),
22 10064–10071. <https://doi.org/10.1073/pnas.1901730116>.
- 23 (77) Zhao, X.; Drlica, K. Reactive Oxygen Species and the Bacterial Response to Lethal
24 Stress. *Curr. Opin. Microbiol.* **2014**, *21*, 1–6.

- 1 <https://doi.org/10.1016/j.mib.2014.06.008>.
- 2 (78) Zahir, T.; Pesek, J.; Franke, S.; Van Pee, J.; Rathore, A.; Smeets, B.; Ramon, H.; Xu,
3 X.; Fauvart, M.; Michiels, J. Model-driven Controlled Alteration of Nanopillar Cap
4 Architecture Reveals Its Effects on Bactericidal Activity. *Microorganisms* **2020**, *8* (2),
5 1–16. <https://doi.org/10.3390/microorganisms8020186>.
- 6 (79) Velic, A.; Hasan, J.; Li, Z.; Yarlagaadda, P. K. D. V. Mechanics of Bacterial Interaction
7 and Death on Nanopatterned Surfaces. *Biophys. J.* **2021**, *120* (2), 217–231.
8 <https://doi.org/10.1016/j.bpj.2020.12.003>.
- 9 (80) Stocks, S. M.; Thomas, C. R. Strength of Mid-Logarithmic and Stationary Phase
10 Saccharopolyspora Erythraea Hyphae during a Batch Fermentation in Defined Nitrate-
11 Limited Medium. *Biotechnol. Bioeng.* **2001**, *73* (5), 370–378.
12 <https://doi.org/10.1002/bit.1070>.
- 13 (81) Li, F.; Chan, C. U.; Ohl, C. D. Yield Strength of Human Erythrocyte Membranes to
14 Impulsive Stretching. *Biophys. J.* **2013**, *105* (4), 872–879.
15 <https://doi.org/10.1016/j.bpj.2013.06.045>.
- 16 (82) Thwaites, J. J.; Surana, U. C.; Jones, A. M. Mechanical Properties of Bacillus Subtilis
17 Cell Walls: Effects of Ions and Lysozyme. *J. Bacteriol.* **1991**, *173* (1), 204–210.
18 <https://doi.org/10.1128/jb.173.1.204-210.1991>.
- 19 (83) Tolpekina, T. V.; Den Otter, W. K.; Briels, W. J. Simulations of Stable Pores in
20 Membranes: System Size Dependence and Line Tension. *J. Chem. Phys.* **2004**, *121*
21 (16), 8014–8020. <https://doi.org/10.1063/1.1796254>.
- 22 (84) Thwaites, J. J.; Mendelson, N. H. Biomechanics of Bacterial Walls: Studies of
23 Bacterial Thread Made from Bacillus Subtilis. *Proc. Natl. Acad. Sci. U. S. A.* **1985**, *82*

- 1 (7), 2163–2167. <https://doi.org/10.1073/pnas.82.7.2163>.
- 2 (85) Maleki, E.; Mirzaali, M. J.; Guagliano, M.; Bagherifard, S. Analyzing the Mechano-
3 Bactericidal Effect of Nano-Patterned Surfaces on Different Bacteria Species. *Surf.*
4 *Coatings Technol.* **2021**, *408* (December 2020), 126782.
5 <https://doi.org/10.1016/j.surfcoat.2020.126782>.
- 6 (86) Velic, A.; Tesfamichael, T.; Li, Z.; Yarlalagadda, P. K. D. V. Parametric Study on
7 Nanopattern Bactericidal Activity. *Procedia Manuf.* **2019**, *30*, 514–521.
8 <https://doi.org/10.1016/j.promfg.2019.02.072>.
- 9 (87) Amir, A.; Babaeipour, F.; McIntosh, D. B.; Nelson, D. R.; Jun, S. Bending Forces
10 Plastically Deform Growing Bacterial Cell Walls. *Proc. Natl. Acad. Sci. U. S. A.* **2014**,
11 *111* (16), 5778–5783. <https://doi.org/10.1073/pnas.1317497111>.
- 12 (88) Quignon, B.; Pilkington, G. A.; Thormann, E.; Claesson, P. M.; Ashfold, M. N. R.;
13 Mattia, D.; Leese, H.; Davis, S. A.; Briscoe, W. H. Sustained Frictional Instabilities on
14 Nanodomed Surfaces: Stick-Slip Amplitude Coefficient. *ACS Nano* **2013**, *7* (12),
15 10850–10862. <https://doi.org/10.1021/nn404276p>.
- 16 (89) Pilkington, G. A.; Thormann, E.; Claesson, P. M.; Fuge, G. M.; Fox, O. J. L.; Ashfold,
17 M. N. R.; Leese, H.; Mattia, D.; Briscoe, W. H. Amontonian Frictional Behaviour of
18 Nanostructured Surfaces. *Phys. Chem. Chem. Phys.* **2011**, *13* (20), 9318–9326.
19 <https://doi.org/10.1039/c0cp02657c>.
- 20 (90) Ishak, M. I.; Dobryden, I.; Martin Claesson, P.; Briscoe, W. H.; Su, B. Friction at
21 Nanopillared Polymer Surfaces beyond Amontons' Laws: Stick-Slip Amplitude
22 Coefficient (SSAC) and Multiparametric Nanotribological Properties. *J. Colloid*
23 *Interface Sci.* **2021**, *583*, 414–424. <https://doi.org/10.1016/j.jcis.2020.09.038>.

- 1 (91) Xiao, K.; Cao, X.; Chen, X.; Hu, H.; Wu, C. Bactericidal Efficacy of Nanopatterned
2 Surface Tuned by Topography. *J. Appl. Phys.* **2020**, *128* (6).
3 <https://doi.org/10.1063/5.0010343>.
- 4 (92) Jun, Y.; Tripathy, S. K.; Narayanareddy, B. R. J.; Mattson-Hoss, M. K.; Gross, S. P.
5 Efficiency of Black Silicon Surfaces Corrigendum : In Fluence of Nanoscale
6 Topology on the Bactericidal Efficiency of Black Silicon Surfaces (2017. *Biophys.*
7 *J.* **2014**, *107* (6), 1474–1484.
- 8 (93) Mo, S.; Mehrjou, B.; Tang, K.; Wang, H.; Huo, K.; Qasim, A. M.; Wang, G.; Chu, P.
9 K. Dimensional-Dependent Antibacterial Behavior on Bioactive Micro/Nano
10 Polyetheretherketone (PEEK) Arrays. *Chem. Eng. J.* **2020**, *392* (December 2019),
11 123736. <https://doi.org/10.1016/j.cej.2019.123736>.
- 12 (94) Hochbaum, A. I.; Aizenberg, J. Bacteria Pattern Spontaneously on Periodic
13 Nanostructure Arrays. *Nano Lett.* **2010**, *10* (9), 3717–3721.
14 <https://doi.org/10.1021/nl102290k>.
- 15 (95) Kim, S.; Jung, U. T.; Kim, S. K.; Lee, J. H.; Choi, H. S.; Kim, C. S.; Jeong, M. Y.
16 Nanostructured Multifunctional Surface with Antireflective and Antimicrobial
17 Characteristics. *ACS Appl. Mater. Interfaces* **2015**, *7* (1), 326–331.
18 <https://doi.org/10.1021/am506254r>.
- 19 (96) Ivanova, E. P.; Linklater, D. P.; Werner, M.; Baulin, V. A.; Xu, X. M.; Vrancken, N.;
20 Rubanov, S.; Hanssen, E.; Wandiyanto, J.; Truong, V. K.; Elbourne, A.; Maclaughlin,
21 S.; Juodkazis, S.; Crawford, R. J. The Multi-Faceted Mechano-Bactericidal
22 Mechanism of Nanostructured Surfaces. *Proc. Natl. Acad. Sci. U. S. A.* **2020**, *117* (23),
23 12598–12605. <https://doi.org/10.1073/pnas.1916680117>.
- 24 (97) Sahoo, P. K.; Janissen, R.; Monteiro, M. P.; Cavalli, A.; Murillo, D. M.; Merfa, M. V.;

- 1 Cesar, C. L.; Carvalho, H. F.; De Souza, A. A.; Bakkers, E. P. A. M.; Cotta, M. A.
2 Nanowire Arrays as Cell Force Sensors to Investigate Adhesion-Enhanced Holdfast of
3 Single Cell Bacteria and Biofilm Stability. *Nano Lett.* **2016**, *16* (7), 4656–4664.
4 <https://doi.org/10.1021/acs.nanolett.6b01998>.
- 5 (98) Jeong, H. E.; Kim, I.; Karam, P.; Choi, H. J.; Yang, P. Bacterial Recognition of Silicon
6 Nanowire Arrays. *Nano Lett.* **2013**, *13* (6), 2864–2869.
7 <https://doi.org/10.1021/nl401205b>.
- 8 (99) Chen, C.; Enrico, A.; Pettersson, T.; Ek, M.; Herland, A.; Niklaus, F.; Stemme, G.;
9 Wågberg, L. Bactericidal Surfaces Prepared by Femtosecond Laser Patterning and
10 Layer-by-Layer Polyelectrolyte Coating. *J. Colloid Interface Sci.* **2020**, *575*, 286–297.
11 <https://doi.org/10.1016/j.jcis.2020.04.107>.
- 12 (100) Kelleher, S. M.; Habimana, O.; Lawler, J.; Reilly, B. O.; Daniels, S.; Casey, E.;
13 Cowley, A. Cicada Wing Surface Topography : An Investigation into the Bactericidal
14 Properties of Nanostructural Features. *ACS Appl. Mater. Interfaces* **2015**.
15 <https://doi.org/10.1021/acsami.5b08309>.
- 16 (101) Ganjian, M.; Angeloni, L.; Mirzaali, M. J.; Modaresifar, K.; Hagen, C. W.; Ghatkesar,
17 M. K.; Hagedoorn, P. L.; Fratila-Apachitei, L. E.; Zadpoor, A. A. Quantitative
18 Mechanics of 3D Printed Nanopillars Interacting with Bacterial Cells. *Nanoscale* **2020**,
19 *12* (43), 21988–22001. <https://doi.org/10.1039/d0nr05984f>.
- 20 (102) Linklater, D. P.; De Volder, M.; Baulin, V. A.; Werner, M.; Jessl, S.; Golozar, M.;
21 Maggini, L.; Rubanov, S.; Hanssen, E.; Juodkazis, S.; Ivanova, E. P. High Aspect
22 Ratio Nanostructures Kill Bacteria via Storage and Release of Mechanical Energy.
23 *ACS Nano* **2018**, *12* (7), 6657–6667. <https://doi.org/10.1021/acs.nano.8b01665>.
- 24 (103) Shahali, H.; Hasan, J.; Mathews, A.; Wang, H.; Yan, C.; Tesfamichael, T.;

- 1 Yarlagadda, P. K. D. V. Multi-Biofunctional Properties of Three Species of Cicada
2 Wings and Biomimetic Fabrication of Nanopatterned Titanium Pillars. *J. Mater.*
3 *Chem. B* **2019**, 7 (8), 1300–1310. <https://doi.org/10.1039/C8TB03295E>.
- 4 (104) Modaresifar, K.; Azizian, S.; Ganjian, M.; Fratila-Apachitei, L. E.; Zadpoor, A. A.
5 Bactericidal Effects of Nanopatterns: A Systematic Review. *Acta Biomater.* **2019**, 83,
6 29–36. <https://doi.org/10.1016/j.actbio.2018.09.059>.
- 7 (105) Silhavy, T. J.; Kahne, D.; Walker, S. The Bacterial Cell Envelope. *Cold Spring Harb*
8 *Perspect Biol* **2010**, 2, 1–16. <https://doi.org/10.1101/cshperspect.a000414>.
- 9 (106) Diu, T.; Faruqui, N.; Sjöström, T.; Lamarre, B.; Jenkinson, H. F.; Su, B.; Ryadnov, M.
10 G. Cicada-Inspired Cell-Instructive Nanopatterned Arrays. *Sci. Rep.* **2014**, 4,
11 <https://doi.org/10.1038/srep07122>.
- 12 (107) Truong, V. K.; Geeganagamage, N. M.; Baulin, V. A.; Vongsvivut, J.; Tobin, M. J.;
13 Luque, P.; Crawford, R. J.; Ivanova, E. P. The Susceptibility of Staphylococcus
14 Aureus CIP 65.8 and Pseudomonas Aeruginosa ATCC 9721 Cells to the Bactericidal
15 Action of Nanostructured Calopteryx Haemorrhoidalis Damselyfly Wing Surfaces.
16 *Appl. Microbiol. Biotechnol.* **2017**, 101 (11), 4683–4690.
17 <https://doi.org/10.1007/s00253-017-8205-9>.
- 18 (108) Hasan, J.; Jain, S.; Chatterjee, K. Nanoscale Topography on Black Titanium Imparts
19 Multi-Biofunctional Properties for Orthopedic Applications. *Sci. Rep.* **2017**, 7
20 (January), 1–13. <https://doi.org/10.1038/srep41118>.
- 21 (109) Martel-Frchet, V.; Ivanova, E. P.; Le Clainche, T.; Linklater, D.; Wong, S.; Le, P.;
22 Juodkazis, S.; Le Guevel, X.; Coll, J. L. Mechano-Bactericidal Titanium Surfaces for
23 Bone Tissue Engineering. *ACS Appl. Mater. Interfaces* **2020**, 12 (43), 48272–48283.
24 <https://doi.org/10.1021/acsami.0c11502>.

- 1 (110) Bhadra, C. M.; Khanh Truong, V.; Pham, V. T. H.; Al Kobaisi, M.; Seniutinas, G.;
2 Wang, J. Y.; Juodkazis, S.; Crawford, R. J.; Ivanova, E. P. Antibacterial Titanium
3 Nano-Patterned Arrays Inspired by Dragonfly Wings. *Sci. Rep.* **2015**, *5*, 1–12.
4 <https://doi.org/10.1038/srep16817>.
- 5 (111) Modaresifar, K.; Ganjian, M.; Angeloni, L.; Minneboo, M.; Ghatkesar, M. K.;
6 Hagedoorn, P. L.; Fratila-Apachitei, L. E.; Zadpoor, A. A. On the Use of Black Ti as a
7 Bone Substituting Biomaterial: Behind the Scenes of Dual-Functionality. *Small* **2021**,
8 *17* (24), 1–15. <https://doi.org/10.1002/sml.202100706>.
- 9 (112) Azeredo, J.; Visser, J.; Oliveira, R. Exopolymers in Bacterial Adhesion: Interpretation
10 in Terms of DLVO and XDLVO Theories. *Colloids Surfaces B Biointerfaces* **1999**, *14*
11 (1–4), 141–148. [https://doi.org/10.1016/S0927-7765\(99\)00031-4](https://doi.org/10.1016/S0927-7765(99)00031-4).
- 12 (113) Krasowska, A.; Sigler, K. How Microorganisms Use Hydrophobicity and What Does
13 This Mean for Human Needs? *Front. Cell. Infect. Microbiol.* **2014**, *4* (AUG), 1–7.
14 <https://doi.org/10.3389/fcimb.2014.00112>.
- 15 (114) Wandiyanto, J. V.; Tamanna, T.; Linklater, D. P.; Truong, V. K.; Al Kobaisi, M.;
16 Baulin, V. A.; Joudkazis, S.; Thissen, H.; Crawford, R. J.; Ivanova, E. P. Tunable
17 Morphological Changes of Asymmetric Titanium Nanosheets with Bactericidal
18 Properties. *J. Colloid Interface Sci.* **2020**, *560*, 572–580.
19 <https://doi.org/10.1016/j.jcis.2019.10.067>.

20

21

22